Towards Practical Application of Gasification: A Critical Review from Syngas and Biochar Perspectives

Siming You[1,2], Yong Sik Ok[3], Daniel C.W. Tsang[4], Eilhann E. Kwon[5], Chi-Hwa Wang[6*]

[1]NUS Environmental Research Institute, National University of Singapore, Singapore 138602, Singapore.

[2]Division of Systems, Power & Energy, School of Engineering, University of Glasgow, G12 8QQ.

[3]Korea Biochar Research Center, O-Jeong Eco-Resilience Institute & Division of Environmental Science and Ecological Engineering, Korea University, Seoul, Korea.

[4]Department of Civil and Environmental Engineering, Hong Kong Polytechnic University, Hung Hom, Kowloon, Hong Kong, China.

[5]Department of Energy and Environment, Sejong University, Seoul 05006, Korea.

[6]Department of Chemical and Biomolecular Engineering, National University of Singapore, Singapore 117585, Singapore.

Re-submitted to

Critical Reviews in Environmental Science and Technology

*Corresponding Author. Tel: +65 65165079; Fax: +65 67791936;

Email: chewch@nus.edu.sg (C. H. Wang)

ABSTRACT

Syngas and biochar production are mainly influenced by temperature, feedstock properties, gasifying agent, pressure, and the mass ratio between gasifying agent and feedstock with temperature being the most significant factor. Increasing temperature generally promotes syngas production while suppressing biochar production. The selection of gasifiers (fixed bed, fluidized bed, and entrained flow) is highly dependent on scale requirement (*e.g.*, volume of feedstock and energy demand), feedstock characteristics (*e.g.*, moisture and ash content), and the quality of syngas and biochar. Updraft fixed bed gasifiers are suitable for the feedstocks with a moisture content up to 50 wt.%. High ash feedstocks such as Indian coal, dried sewage sludge, and municipal solid waste that are not suitable for fixed bed gasifiers, have been successfully gasified in bubbling fluidized bed reactors. Woody biomass is not suitable for entrained flow gasifiers unless specialized feeding methods are employed such as wood torrefaction and grinding followed by the existing feeding methods for pulverized coals, biomass-oil biochar slurry preparation followed by pumping, wood or torrefied wood slurry preparation followed by pumping, *etc*. Syngas and biochar can potentially be contaminated by NH_3, H_2S, and tar, which can be removed using catalysts (*e.g.*, Ni-based), metal oxides-based sorbents, and thermal and catalytic cracking methods. Existing syngas and biochar upgrading methods suffered from various problems such as economic infeasibility, limited productivity, and fouling, and future syngas and biochar upgrading methods should be aimed to have the features of reliability, security, affordability, and sustainability, towards the practical, large-scale production of syngas- and biochar-based products. One potential solution is to develop integrated systems by combining biochar upgrading and application with syngas upgrading, which warrants an integrated perspective based on both life cycle assessment and economic analysis.

Keywords: Syngas; Black carbon; Pyrolysis/Gasification; Biofuel; Biorefinery; Catalysts.

1 INTRODUCTION

The gasification technology has been used as an eco-friendly means to dispose of most carbonaceous materials such as waste biomass and municipal solid waste (MSW) which are posing a grand environmental benefit to megacities. Compared to landfill and incineration, gasification is featured by its higher energy recovery efficiency, lower environmental pollutant emissions, and enhanced flexibility for waste management via decentralized applications at the source of homogeneous industrial/agricultural waste streams (Buragohain et al., 2010; Maya et al., 2016). Meanwhile, gasification is differentiated from other thermochemical processes (*e.g.*, slow and fast pyrolysis), as well as torrefaction, by its relatively high reaction temperature (> 500 °C), moderate heating rate (a few to tens of °C/min except for some entrained flow gasification cases where high heating rates (10^3 - 10^4 °C/s) were intentionally applied (Liu et al., 2003; Tremel et al., 2012b; Wang et al., 2005)) and moderate reaction pressure (atmospheric to several tenths of MPa) as shown in Figure 1.

As the primary product of gasification, syngas is a mixture of product gases mainly consisting of carbon monoxide (CO), hydrogen (H_2), carbon dioxide (CO_2), and methane (CH_4), which can be catalytically converted into liquid fuel (*i.e.*, Fischer-Tropsch), value-added chemicals (*e.g.*, ammonia, methanol), or directly used as a fuel for power generation (Asthana et al., 2017; Lee et al., 2017b; Wang et al., 2017). The H_2 production from the gasification of biomass has received particular interest because of its relatively high efficiency (>50%) and eco-friendly nature (Hosseinpour et al., 2017; Moneti et al., 2016; Parthasarathy & Narayanan, 2014; Yao et al., 2016). Moreover, the cost of the H_2 production from biomass gasification was

$14 - 25 /GJ, which was lower than that from wind-, solar-, and nuclear-based methods (Balat & Kırtay, 2010).

Byproduct of gasification, *i.e.*, biochar, has been increasingly studied in the last decade, because of its versatile application possibilities such as soil amendment for carbon sequestration, catalyst for tar removal, a precursor of adsorbent, *etc* (Inyang et al., 2016; Rajapaksha et al., 2016; Xiong et al., 2017; You et al., 2017a). Emerging knowledge and evidence on the commercialization and applications of biochar suggest that the valorization of biochar can potentially improve the overall economic and environmental values of a gasification system. Hence, it is desirable to have a systematic perspective considering the application and valorization of both syngas and biochar for designing economically and environmentally sustainable gasification systems. This suggests the importance of accurately engineering the properties and yield of syngas and biochar according to the requirements designated by a specific application.

An overview of the gasification technology in terms of both syngas and biochar production is warranted to assist optimum design and planning of gasification systems. This review focuses on: (i) understanding the thermochemical principles of gasification and their relationships with syngas and biochar production; (ii) differentiating various types of gasifiers in terms of their design, operation, and production characteristics; (iii) evaluating the contamination issues related to syngas and biochar during the gasification process; (iv) exploring the existing methods of upgrading syngas and biochar for better commercial utilization; (v) discussing the potential and future research and development directions of gasification.

2 GASIFICATION AND GASIFIERS

2.1 Thermochemical principles

A gasification process generally involves a sequence of four reaction stages, *i.e.*, drying, pyrolysis, combustion, and reduction. There are often overlaps between the reactions of the stages, making boundaries between them un-differentiable.

2.1.1 Drying

The drying stage involves the evaporation of free and bound water in the feedstock by the heat from the exothermic reactions (*e.g.*, partial and/or complete oxidation) in the subsequent stages. The temperature is generally between 100 and 200 °C, which is not enough to thermally decompose the feedstock (Patra & Sheth, 2015; Udomsirichakorn & Salam, 2014). However, the drying process may release some air pollutants such as volatile organic compounds (*e.g.*, terpenes) (McKendry, 2002). High moisture content in the feedstock not only leads to feeding or fluidization problems such as jamming and agglomerate formation but also decreases the lower heating value (LHV) of product gas and thus the overall energy efficiency of gasification, and increase the tar content in syngas as a result of the decrease in reaction temperature (Aziz et al., 2015; Kaewluan & Pipatmanomai, 2011). For high-moisture feedstocks, a drying pretreatment is needed prior to gasification (You et al., 2016). However, it is worth noting that an appropriate range of moisture content in feedstocks may indirectly enhance the biochar production because of the decrease in gasification efficiency, which is attributed to the fact that a significant amount of heat is consumed by the evaporation of moisture content and thus the rise of temperature inside a reactor is inhibited (Prins et al., 2006; Rezaei et al., 2016). The drying rate is mainly dictated by the heat and mass transfer between feedstock particles and their surrounding atmosphere which is associated with the particle surface area, temperature

difference, moisture and convection velocity of surrounding flows, and diffusivity of moisture within feedstock particles (Dogru et al., 2002; Liu et al., 2013).

2.1.2 Pyrolysis

During pyrolysis, the feedstock particles are decomposed into volatile matter and carbonaceous solid residue (biochar) under increased temperatures. Some of the volatile species in the cooler part of feedstock condense and produce tar (Sheth & Babu, 2009). The reactions of this stage do not involve oxygen (oxygen is not utilized until subsequent oxidization and reduction stages) and the stage is generally conducted from 200 to 700, 300 to 800, and 600 to 1600 °C for fixed bed, fluidized bed, and entrained flow reactors, respectively (Arena, 2012; Kim et al., 2012; Newalkar et al., 2014; Park et al., 2014; Patra & Sheth, 2015; Sanchez-Silva et al., 2012; Shen et al., 2015b; Tanner et al., 2015; Tremel et al., 2012a; Xue et al., 2015). Biochar is the primary product of pyrolysis after the depletion of volatile matter. The production and properties of pyrolysis biochar are affected by various operating parameters such as pyrolysis temperature, pressure, heating rate, feedstock residence in the pyrolysis zone, physical and chemical properties of feedstock (*e.g.*, particle size and compositions), as well as gasifier configurations (Ceylan & Topçu, 2014; Erkiaga et al., 2014; Manyà, 2012). The thermochemical conditions (*e.g.*, temperature, residence time, and heating rate) have major effects on the surface area and pH of pyrolysis biochar, while the properties of feedstock determine the carbon and ash contents (Ronsse et al., 2013; Zhao et al., 2013a).

In general, under a higher pyrolysis temperature, more gaseous volatile matter are released which facilitate the formation of micropores and increase the specific surface area of biochar (Kumar et al., 2017b). Increasing the temperature from 450 to 600 ^{o}C increased the specific surface area of pyrolysis biochar by 30 times for a variety of feedstocks including hickory wood, bagasse, and bamboo (Sun et al., 2014). A similar magnitude of increase was found

when the temperature was increased from 450 to 500 ^{o}C during the pyrolysis of Geodae-Uksae (Lee et al., 2013b). Suliman et al. (2016) observed a three-fold increase in the specific surface area of biochar as the pyrolysis temperature increased from 350 to 600 ^{o}C for Douglas fir wood, Douglas fir bark, and hybrid poplar wood, which was attributed to the formation of micropores. The pyrolysis temperature was the most influential parameter affecting the specific surface area of rapeseed stem biochar: the area increased from 1 to 45 m^2/g as the pyrolysis temperature increased from 200 to 700 °C (Zhao et al., 2018).

Mohan et al. (2014) noted that high heating rates reduced the specific surface area and pore volume of biochar due to rapid depolymerization at the biochar surfaces. However, Chen et al. (2014) found that increasing the heating rate from 5 to 30 ^{o}C/min increased the specific surface area of pyrolysis biochar from 64 to 72 m^2/g. Zhao et al. (2018) found that the specific surface area of rapeseed stem biochar was increased by approximately 30% as the heating rate increased from 1 to 20 °C/min, due to the enhanced process of thermal decomposition. Zhao et al. (2018) also found that the specific surface area firstly increased as the residence time increased from 10 to 60 min due to a greater destruction of the cellular structure of biomass, then slightly decreased as it increased from 60 to 100 min.

The fixed carbon content of the biochar generally increased with the increase of pyrolysis temperature, partly because of the increased loss of volatile matter (Manyà, 2012). However, the yield of pyrolysis biochar generally decreases with the increase in temperature and heating rate. For example, increasing the heating rate from 10 to 50 °C/min and temperature from 400 to 600 °C decreased the yield of safflower seed biochar by 3 - 8% (Angın, 2013). An increase in pressure enhances the biochar yield from pyrolysis because the increased vapor residence time within feedstock particles promotes char forming reactions by extending vapor-solid contact (Mohan et al., 2014). The specific surface area of biochar decreased as the pressure increased. This is because micropores were clogged by the melting and trapping of volatile

matter and even collapsed under a high pressure condition (Cetin et al., 2005; Melligan et al., 2011). High moisture and lignin contents in feedstocks also promoted the yield of pyrolysis biochar under the condition of elevated pressures (Manyà, 2012). High-pressure gasification has the advantages of favoring product gas clean-up by imposing a high pressure drop in cleaning units such as cyclones and filters, saving the syngas compression energy and operating cost (syngas may be directly fed into a gas turbine without further compression), and facilitating equipment size reduction and some post-stream upgrading processes such as methanol synthesis (>5 MPa) (Chmielniak & Sciazko, 2003; Craven et al., 2014). However, it is worth noting that the typical disadvantages of high-pressure gasification include additional effort required to maintain a steady pressure conditions, feeding problems at high pressure, and potential risks related to the gas leakage at high pressure (Sweeney, 2012).

As an amorphous and hydrophobic polymer, lignin has a high molecular weight larger than 10000 g/mol and consists of numerous functional groups with aromatic sub-structures of carbon whose decomposition produces condensed aromatic carbons with reduced functional groups and contributes to the formation of biochar (Lee et al., 2013a). The yield of pyrolysis biochar is also increased by the increase of feedstock particle size, which is because (1) the smaller surface area of larger feedstock particles reduces the overall reaction rate of the particles, and (2) the decreasing volatile diffusion rate through biochar increases the retention time of volatile species, which enhances the secondary charring reactions between tar vapors and solid matrix and thus the formation of recalcitrant biochar (Anca-Couce et al., 2014; Demirbas, 2004; Manyà et al., 2007).

Alkali and alkaline earth metallic (AAEM) species (*e.g.*, K, Na, Ca, Mg, and Fe) are ubiquitous elements in biomass, which can serve as a catalyst for pyrolysis. The presence of these elements in feedstocks enhances feedstock decomposition and char-forming reactions during pyrolysis (Chen & Yang, 1997; Li et al., 2000). Removing AAEM species by acid

pretreatment was regarded as an effective way to improve the yield of bio-oil from pyrolysis, but gas production was also mitigated particularly by the removal of K that catalyzed the decarbonylation and decarboxylation reactions of pyrolysis vapors (Hernando et al., 2016). The ion-exchangeable AAEM species, particularly Na^{+}, Mg^{2+} and Ca^{2+} in the brown coal were closely related to the formation rates and yields of light hydrocarbons, oxygen-containing species, biochar, and tar during pyrolysis (Li, 2007; Quyn et al., 2002). The biochar generated during the pyrolysis stage is subjected to additional thermochemical treatment during the subsequent stages (combustion and reduction), where the compositions, surface morphology, fixed carbon aromaticity, and other chemical properties of biochar go through further modifications (Patra & Sheth, 2015).

2.1.3 Combustion

This stage involves the complete or partial oxidation of carbonaceous materials and some pyrolysis gas species (CO, H_2, CH_4 and C_nH_m), producing H_2O, CO_2, and CO. This exothermic oxidation stage usually takes place in a temperature range from 700 to 1500 °C (Patra & Sheth, 2015), and supplies heat to the endothermic drying process as well as pyrolysis and reduction reactions (Dogru et al., 2002; Simone et al., 2013). Under a high temperature from 900 to 1100 °C, some heavy molecules are broken down to lighter molecules, and some of the tar is thermally cracked (Di Blasi & Branca, 2013; McKendry, 2002; Patra & Sheth, 2015). The major reactions (at 25 ^{o}C) of the combustion stage include:

$$\text{Carbon partial oxidation: } C\ (s) + \tfrac{1}{2}\ O_2\ (g) \rightarrow CO\ (g)\ (\Delta H = -111\ kJ\ mol^{-1}) \quad (1)$$

$$\text{Carbon complete oxidation } C\ (s) + O_2\ (g) \rightarrow CO_2\ (g)\ (\Delta H = -394\ kJ\ mol^{-1}) \quad (2)$$

$$\text{Gas oxidation: } H_2\ (g) + \tfrac{1}{2}\ O_2\ (g) \rightarrow H_2O\ (g)\ (\Delta H = -242\ kJ\ mol^{-1})$$

$$CO\ (g) + \tfrac{1}{2}\ O_2\ (g) \rightarrow CO_2\ (g)\ (\Delta H = -283\ kJ\ mol^{-1}) \quad (3)$$

CH_4 (g) + ½ O_2 (g) → CO (g) + $2H_2$ (g) (ΔH=-35.7 kJ mol^{-1})

The oxidation of volatile gases (*i.e.*, gas oxidation reactions (Eq. (3))) takes place so fast that most of the oxygen is used up before diffusing to the surface of the biochar, mitigating biochar oxidation (Eq. (1) and (2)) (Dogru et al., 2002). Under a sub-stoichiometric oxygen condition, partial oxidization of carbon is dominant and produces CO (Eq. (1)). The steam produced by combustion serves as the reactant of the water gas reaction and water gas shift reaction during the subsequent reduction stage. Not all biochar is consumed by the heterogeneous oxidization reactions due to the oxygen-deficient condition and the remaining serves as the reactant of the Boudouard reaction and water gas reaction during the subsequent reduction stage.

2.1.4 Reduction

Reduction takes place in a temperature range of 800 - 1000 °C (Patra & Sheth, 2015). During the reduction stage, the biochar reacts with H_2O, CO_2, and H_2 to produce a mixture of combustible gases such as CO, H_2, CH_4, and light hydrocarbons such as acetylene and ethylene. Main reduction reactions (at 25 °C) include (Puig-Arnavat et al., 2010):

Boudouard reaction: C (s) + CO_2 (g) → 2CO (g) (ΔH=+172 kJ mol^{-1}) (4)

Water gas reaction: C (s) + H_2O (g) → CO (g) + H_2 (g) (ΔH=+131 kJ mol^{-1}) (5)

Water gas shift reaction: CO (g) + H_2O (g) ↔ CO_2 (g) + H_2 (g) (ΔH=-41 kJ mol^{-1}) (6)

Methane reaction C (s) + $2H_2$ (g) → CH_4 (g) (ΔH=-75 kJ mol^{-1}) (7)

In general, the biochar reaction with H_2O is faster than the biochar reaction with CO_2 (Nilsson et al., 2013). The reaction rates of Eq. (1), Eq. (4), and Eq. (5) can be expressed as $2.3T_s e^{-\frac{11100}{T_s}}$, $589T_s e^{-\frac{26800}{T_s}}$ and $5.714T_s e^{-\frac{15600}{T_s}}$, respectively, with T_s being the biochar particle temperature (Yao et al., 2018). Based on these expressions, the reaction rate of the water gas reaction (Eq.

(5)) can be one order of magnitude larger than that of the Boudouard reaction (Eq. (4)) but a few tenths of that of the partial oxidization reaction (Eq. (1)), under the condition that T_s is lower than 2000 ^{o}C.

The thermal energy in the gas phase supports the propagation of the reduction reactions, and some of the energy is transferred to the solid phases until the thermal equilibrium is reached (Tinaut et al., 2008). The heat transfer between the two phases is enhanced upon the gradual consumption of carbon (Eq. (5)) that increases the contact area between the gas and solid phase. Under the equilibrium condition, the chemical reactions are held at fixed rates and the temperature of solid and gas phases diminish by the heat transfer via the gasifier wall. The reaction rates have been regarded to have an Arrhenius type temperature dependence and were proportional to the difference between the ratio of reactant to product and the equilibrium ratio (Babu & Sheth, 2006; Huang et al., 2010; Muroyama & Loutzenhiser, 2016). The reduction reactions are usually much slower than the combustion reactions (Di Blasi, 2009). However, the oxygen-deficient condition in a gasifier favors the reduction reactions, so that they dominate over the combustion reactions. The influential factors of the reduction stage include the temperature, feedstock properties, gasifying agent, pressure, and the ratio between gasifying agent and feedstock (Cha et al., 2016). Similar to pyrolysis, temperature is still the most significant factor, and increasing temperature promotes the production of H_2 and CO and reduces the production of CO_2 and CH_4, hydrocarbons, and tar (Gómez-Barea et al., 2013; Taba et al., 2012). Due to the endothermic nature of the reduction reactions (Boudouard and water gas reactors), the carbon conversion efficiency (*i.e.*, the ratio of the carbon mass flow in product gas to the initial carbon mass in feedstock), and reaction rate increase as the temperature and partial pressure of gasifying agents increase. For example, based on a volumetric model, Aranda et al. (2016) found that the reaction rate increased from 0.0108, 0.0147, and 0.0153 min^{-1} to 0.0198, 0.0473, and 0.0824 min^{-1} when the temperature increased from 800 to 900 ^{o}C

under the steam pressure of 0.02, 0.05, and 0.07 MPa, respectively for steam gasification of Indian high-ash coal in a fluidized bed reactor. Under the same temperature (*e.g.*, 800 ^{o}C), the reaction rate increased from 0.018 to 0.0153 min^{-1}, when the steam pressure increased from 0.02 to 0.07 MPa. Wang et al. (2016) found that the reaction rate of CO_2 gasification of biomass chars increased from 0.0186 – 0.036 min^{-1} to 0.1104 – 0.3486 min^{-1} as the temperature increased from 850 to 1000 ^{o}C at atmospheric pressure.

Rollinson (2016) found that a higher moisture content in pine wood decreased the CO content but increased the CO_2 content in the product gas, because the higher moisture content lowered the temperature of the reduction zone via the evaporation of H_2O that favored the exothermic water gas shift (WGS) reaction (Eq. (6)) and suppressed the endothermic reactions (Eq. (4) and Eq. (5)). Consequently, the heating value of the product gas decreased as the pine wood moisture content increased. The biochar from the pine wood with the moisture of 7 wt.% had 27% more fixed carbon content (on a dry basis), 45% less ash content (on a dry basis), 60% larger specific surface area, 67% larger micropore volume, and 62% larger micropore area than that from the feedstock with the moisture of 17 wt. % (Rollinson, 2016). Furthermore, the biochar from the lower moisture pine wood contained a higher concentration (187 $\mu g\ g^{-1}$) of 16 priority polycyclic aromatic hydrocarbons (PAHs) than that (89 $\mu g\ g^{-1}$) from the higher moisture pine wood. James R et al. (2016) found that increasing the feedstock moisture content from 10 to 22 wt.% reduced the yields of biochar, tar, and syngas from 12 to 9.9 wt.%, 12.9 to 6.2 g/m^3, and 37.5 to 32.6 vol. %, respectively.

Gasifying agents affect the carbon conversion efficiency, the composition and heating value of product gas, and the physical and chemical properties of gasification biochar. Typical gasifying agents include steam, air, O_2, CO_2, and a mixture of them (Cho et al., 2017b). Due to its natural availability, air is the most common gasifying agent. But it suffers from the disadvantage of lowering the heating value of product gas by introducing extra nitrogen content

(Puig-Arnavat et al., 2010). The heating value of syngas was reported to fall in the range of 3 - 7 MJ/Nm^3 under the gasifying agent of air, compared to 14 - 28 MJ/Nm^3, 3 - 16 MJ/Nm^3, and 5 - 18 MJ/Nm^3 under the gasifying agent of pure oxygen, steam, and carbon dioxide, respectively (Chen et al., 2015; Ciferno & Marano, 2002; Fernandez-Lopez et al., 2017; Gujar et al., 2014; Gül et al., 2018; Kumar et al., 2009; Patil et al., 2011; Yao et al., 2017). The wide variation of the syngas heating values for the same agent is associated with the change in the mass ratio between gasifying agent and biomass (or fixed carbon), as well as the change in the reaction temperature. The heating value of syngas increased by 4 - 5 times as the mass ratio decreased from 2.1 to 0.1 for the cases of steam and carbon dioxide gasification (Fernandez-Lopez et al., 2017). Under the condition of CO_2/C=1, increasing the reaction temperature of CO_2 from 800 to 1000 ^oC increased the syngas heating value from around 14 to 16 MJ/Nm^3 (Yao et al., 2017). In addition, CO_2 is commonly used together with a catalyst to promote the conversion of biochar, tar, and methane into syngas (Lahijani et al., 2013; Oh et al., 2017; Ollero et al., 2003).

An external heat source is often needed when steam or CO_2 is used as the gasifying agent because of the allothermic nature of the reactions (Iliuta et al., 2010; Lee et al., 2017a; Pfeifer et al., 2011). In this case, air or O_2 can be added to produce heat from the oxidation reactions. Tay et al. (2013) compared the structures and reactivity of Victorian brown coal biochar under three different gasification atmospheres: 15% H_2O with argon, 4000 ppm O_2 with CO_2, and 4000 ppm O_2 + 15% H_2O with CO_2. The H_2O content in the gasifying agent decreased the relative ratio between small (< 6 fused rings) and large aromatic ring structures, and significantly improved the retention of alkaline metals (Mg and Ca) by changing the physicochemical forms of Mg and Ca. This was possibly because H_2O was dissociated during its reaction with biochar and formed hydrogen radical species, which penetrated the biochar matrix to activate the inner structure of biochar and induce the aromatic ring condensation. The

reduction process using steam or CO_2 as the gasifying agent was similar to the physical activation processes that were used to produce activated carbons (Lee et al., 2017c; Manyà, 2012; Xiu et al., 2017). Hence, the reduction stage using steam or CO_2 serves as an activation step to increase the specific surface area and micropore volume of the biochar, despite that the improvement in the surface properties corresponds to a loss in carbon sequestration capacity (Cho et al., 2017a; Manyà, 2012).

For rice straw gasification, the syngas yield decreased and H_2/CO ratio increased as the air-to-biomass ratio increased, decreasing the cold gas efficiency (*i.e.*, the ratio of the combustion energy of product gas to the input energy), when a mixture of steam and air was used as the gasifying agent (Im-orb et al., 2016). This was because increasing air mass introduced more N_2 and promoted the combustion reaction by adding more oxygen. In contrast, the syngas yield increased and H_2/CO ratio decreased as the CO_2/biomass ratio increased, increasing the cold gas efficiency (Im-orb et al., 2016), when a mixture of steam and CO_2 was used as the gasifying agent. This was attributed to the fact that increasing the CO_2/biomass ratio promoted the Boudouard reaction and the reverse water gas shift reaction, which increased and decreased the concentrations of CO and H_2, respectively.

The gasification reactions are also affected by the flow rate of gasifying agent. Kim et al. (2016) showed that sewage sludge briquettes gasification biochar had larger sizes and higher ash content than the wood pellets gasification biochar. Increasing the air flow rate made the reactions less fuel-rich for the case of sewage sludge, which slowed the propagation speed of ignition front to fresh sewage sludge particles and reduced the decomposition rate of particles. This was further reflected by an increase in the stoichiometric ratio and decreases in the energy content of product gas and biochar production. On the contrary, the reactions for the case of wood pellet became more fuel-rich as the air flow rate increased due to the accelerated pyrolysis and release of volatile matter. The biochar yield from switchgrass gasification at

750 °C decreased from 19 to 7 wt.% as the equivalence ratio (*i.e.*, the ratio of the amount of actual air supply and the stoichiometric amount of air.) increased from 0 to 0.4 (Broer & Brown, 2015). When the equivalence ratio increased from 0 to 0.15, the biochar yield from the gasification of Miscanthus decreased from 30 to 15 wt.% and 25 to 10 wt.% at 700 and 800 °C, respectively (Vriesman et al., 2000).

The presence of AAEM species in the original feedstock may enhance the syngas production and biochar decomposition, because the AAEM species serve as the catalysts of gasification (Xiong et al., 2017). On the other hand, a high content of Si, Al, and P inhibited the reduction process, decreased the yield of syngas, and increased the yield biochar (Gai et al., 2016; Hognon et al., 2014; Jiang et al., 2015; Nzihou & Stanmore, 2013).

2.2 Types of gasifiers

Commonly used gasifiers can be categorized into three major types: fixed bed, fluidized bed, and entrained flow. The selection of gasifiers is contingent upon scale requirement (*e.g.*, volume of feedstock and energy demand), feedstock characteristics (*e.g.*, moisture and ash content), and the quality of syngas and biochar, which is critical for designing techno-economically feasible and environmentally sustainable gasification systems. The scale design of a gasification system is highly contingent on the waste or biomass for disposal and energy demand (Balat et al., 2009). For example, You et al. (2016) designed decentralized gasification systems based on the quantity of sewage sludge and food waste. Shabbir & Mirzaeian (2016) studied gasification-based cogeneration systems based on the thermal demand and maximization of electricity output in a mill. Lythcke-Jørgensen et al. (2017) optimized a multi-generation system consisting of a methanol biorefinery, a gasification-based combined heat and power unit, and an industrial energy utility supply based on economic performance, carbon

footprint, the demand of local district heating, and the thermal utility of the butchery in the Danish city of Horsens.

2.2.1 Fixed bed

Fixed bed gasifiers are typically more suitable for small-scale (10 kW - 10 MW), decentralized applications because of their simple configuration and cost-efficiency under small-scale conditions (Klimantos et al., 2009). In a fixed bed gasifier, the four gasification reaction stages correspond to four stratified temperature zones (Fig. 2 (a) and (b)). Compared to fluidized bed and entrained flow gasifiers, fixed bed gasifiers have poorer heat transfer and mixing of the gas and solids, which result in an uneven radial temperature distribution and various problems such as slagging, bridging, and clinkering in the gasifiers (Beenackers, 1999; Ong et al., 2015). In fixed bed gasifiers, volatile matter released by pyrolysis reactions are ignited by the heat transfer from flames and reactor walls. The ignition front propagates to adjacent fresh particles by heat transfer from the flames formed by the released volatile species, and biochar is combusted and reduced above the ignition front (Kim et al., 2016). The particle size distribution of feedstock affects the bed void ratio, gasifying agent distribution, and pressure drop within the bed (Ryu et al., 2006). Specifically, large feedstock particles created voids and shortcuts (preferential pathways) for the ventilation of gasifying agent within the particle bed, *i.e.*, "channeling" effect, which lead to the differences in oxygen availability among particles and thus the non-uniform temperature distribution. Popular commercial fixed bed gasifiers include British Gas Lurgi (BGL) and Sasol-Lurgi fixed bed dry bottom gasifiers, and both of them had the issues associated with deposits and agglomeration such as the blockage of gas exit and slag tap nozzle, and damage of refractory and tuyeres (Krishnamoorthy & Pisupati, 2015). Based on the relative direction between the gasifying agent and feedstock, fixed bed gasifiers are further divided into updraft and downdraft ones.

(a) Updraft

In an updraft fixed bed gasifier (Fig. 2 (a)), the gasifying agent is introduced from the bottom of reactor and exits from the top, while the feedstock is fed from the top and falls down through the reactor. The reduction zone is above the combustion zone. The hot gas flows upward and enhances the pyrolysis and drying of the descending feedstock, which in turn reduces the reactor's temperature to approximately 500 °C (Chhiti & Kemiha, 2013). Due to the drying enhancement, updraft gasifiers are suitable for feedstocks with moisture content up to 50 wt.% (Mandl et al., 2011).

The product gas leaving the top of the reactor may contain high tar content, and thus updraft gasifiers are not suitable for feedstocks with a high volatile content (Ruiz et al., 2013). The deposited ash has a lower chance to interact with the product gas due to the filtering effect of the bed, and updraft gasifiers are suitable for feedstocks with a high ash content (up to 15 wt.%) (Priyadarsan et al., 2004). Updraft gasifiers also have high thermal efficiencies because of the enhanced heat exchange between the gas flow and descending feedstock (Chen et al., 2013).

(b) Downdraft

In a downdraft fixed bed gasifier (Fig. 2 (b)), the gas is introduced above the reduction zone and flows in the same direction as the descending feedstocks towards the bottom of reactor. The reduction zone is below the combustion zone. Some of the pyrolysis products (gases and biochar) are burnt together with the gasifying agent, supplying heat to the endothermic reactions during the reduction stage. Under a temperature higher than 600 °C in the combustion zone, secondary reactions took place and tars were converted into non-condensable lighter gases (Fagbemi et al., 2001). The relatively high temperature in the combustion stage imposes a thermal cracking effect on the tars, and the resulting product gas contains relatively small

amount (1 g/m^3) of tar (Di Blasi & Branca, 2013; Patra & Sheth, 2015). However, the tar formed in this case was very stable, which led to potential difficulty in down-stream tar removal, if any (Beenackers, 1999). Compared to an updraft fixed bed gasifier, the decarbonization and dehydrogenation reactions in the reduction zone of a downdraft fixed bed gasifier are more efficient (Abioye & Ani, 2015; Zhang et al., 2013). This leads to more carbon consumption and lower ratio of fixed carbon and ash for the biochar for the case of downdraft gasifiers.

The downward flowing of product gas can potentially cause two issues: (1) the upward heat transfer is reduced, which lowers the drying efficiency of feedstock located at the top; (2) the product gas goes through the biochar deposit before leaving the reactor and may be contaminated by particulates. As a result, the feedstocks for downdraft gasifiers should have low moisture (< 25 wt.%) and ash (< 6 wt.%) contents (Table 1) (Guangul et al., 2014; Vera et al., 2018). Feedstocks such as raw food waste, sewage sludge and animal manure with a moisture content well above 50 wt.% (You et al., 2016; Yuan et al., 2017a), and rick husk, palm mesocarp fibers, and wheat straw with an ash content above 10 wt.% (Huang et al., 2016; Pode, 2016; You et al., 2017b) are not suitable for a downdraft fixed bed gasifier. For high moisture feedstocks, a drying pretreatment is needed prior to the gasification of feedstock, which incurs additional energy consumption, operating cost, and logistics requirements to the whole system.

Typical gasification driers are based on the heat from either gasification systems itself or external sources. The waste heat recovery from gasification for drying can serve to enhance system's thermal efficiency. Hot flue gas can be used for rotary driers and steam can be used for fluidized bed driers (McKendry, 2002). Solar energy has been used as an external source of heat for feedstock drying. Natural sun drying is a traditional and cheap way of solar energy utilization. However, it has the disadvantages of humidity re-absorption upon raining and contamination by pathogenic gems, rodents, birds and insects (Ferreira et al., 2008). The

problems related to the natural sun drying can be mitigated by using solar driers which use the solar energy to heat large volumes of air that flows over and dries feedstocks (Murthy, 2009). There are four major types of solar driers, *i.e.*, natural convection cabinet type, forced convection indirect type, greenhouse type, and solar tunnel drier, among which the natural convection greenhouse type driers are highly cost-effective and comparable to open sun drying (Murthy, 2009). For the region without a high solar intensity or with a high relative humidity, mechanical driers such as belt, drum, and vertical tray driers are also available which are heated using kerosene, diesel, or electricity (Werle, 2015b). The mechanical driers are less subject to weather influences.

2.2.2 Fluidized bed

Fluidized bed gasifiers (Fig. 2 (c) and (d)) are featured by the formation of a semi-suspended bed by the upward-flowing gasifying agent fed from the bottom of reactor and are suitable for intermediate scale applications (5 - 100 MW) (Guangul et al., 2012). In the reactor, fresh feedstock particles have a high chance to constantly contact with hot particles due to the suspension of particles, and the overall heat and mass exchange in the reactor is significantly improved. This ensures complete mixing and a uniform temperature distribution, which makes fluidized bed gasifiers applicable for a wide range of feedstocks and particle sizes (Lu et al., 2008; Rapagnà et al., 2010).

The continuous mixing and output of particles, both gasified and partially gasified, means that a fluidized bed reactor cannot achieve a full conversion of biochar (Ruiz et al., 2013). Under atmospheric pressure and a bed temperature lower than 910 °C, the total carbon conversion efficiency in fluidized bed gasifiers ranged from 70 to 85% for an equivalence ratio of 0.2 - 0.3 (Prins et al., 2007). Typical tar content in the product gas of fluidized bed gasifiers ranged from 2 to 20 g/m^3 (Pfeifer et al., 2004). Inertial bed materials are commonly used in

fluidized bed gasifiers, and a post-stream separation process is generally needed to separate biochar particles from the bed materials. Based on the fluidization technique, there are two main types of fluidized-bed gasifiers, *i.e.,* bubbling bed and circulating bed.

(a) Bubbling

In a bubbling fluidized bed gasifier (Fig. 2 (c)), the feedstock is fed from the top while the pressurized gasifying agent is blown upwards through a grate above which a bed of hot materials (*e.g.*, sand or olivine) are placed (Li et al., 2015; Rapagnà et al., 2010). The temperature of the bed material is in a range of 700 - 900 °C, which can decompose some of the high molecular weight tars and reduce the tar content to less than 1 - 3 g/m^3 (Patra & Sheth, 2015; Surisetty et al., 2012). When the devolatilization and oxidant gases were evenly distributed into the emulsion and bubbles, the total tar concentration decreased uniformly as the temperature increased and bed flow-rates decreased (Stark et al., 2016). High ash feedstocks such as Indian coal (36.4 wt.%), dried sewage sludge (43.1 wt.%), and municipal solid waste (44.6 wt.%) have been successfully gasified in bubbling fluidized bed reactors facilitated by fast ash removal (Campoy et al., 2014; Kumar et al., 2017a). However, an excessively high temperature causes problems such as ash melting, sintering, and slagging, especially for the feedstocks with high content of alkali metal oxides whose melting points are relatively low (*e.g.*, 740 ^{o}C for potassium oxide and 1132 ^{o}C for sodium oxide (Haynes, 2014)), and affect the fluidization quality (*i.e.*, defluidization) (Brar et al., 2012).

The excess gas flow relative to the fluidization flow that maintains the minimum fluidization condition leads to the formation of bubbles, and the size of the bubbles is a critical parameter affecting the performance of a bubbling fluidized bed gasifier (Yan et al., 1998). The bubble diameter, bubble velocity, area fraction of bubble, and inter-phase gas transfer rate increased as the increase of temperature but decreased as the increase of bed particle size (Das

& Datta, 2016). The formation of bubbles may affect the oxygen dissemination and limit the combustion of the fluidized particles, which further affect the gasification efficiency (Ruiz et al., 2013). The product gas exits from the top of the reactor and the ash gets drained from the bottom of the bed (Zeng et al., 2016). The enhanced heat and mass exchange increased the overall carbon conversion efficiency, and the quality of biochar is more uniform as a result of the relatively uniform temperature in the gasifier (Surisetty et al., 2012).

(b) Circulating

In a circulating fluidized bed gasifier (Fig. 2 (d)), the feedstock particles move in circulation via a main reaction vessel, cyclone separator, and return leg. The fluidization velocity of circulating bed is higher than that of bubbling bed so that the particles can be suspended across the whole riser height (Loha et al., 2014). The cyclone is used for separating particles from gases while the return leg guides the separated particles back to the reaction vessel from the bottom. In addition to the outer loop circulation of particles, there is an internal circulation in the main reaction vessel corresponding to the upward and downward movement of particles. Due to these re-circulations, the feedstock particles in a circulating fluidized bed gasifier have a significantly longer residence time than that in a bubbling fluidized bed gasifier (Fouilland et al., 2010). The types of bed materials affect the biochar yield by varying the gasification efficiency. For example, the gasification of almond shell on an unmodified olivine bed gave a biochar yield of 4 - 5 % compared to 1 - 1.5% on a Fe/olivine bed (Barisano et al., 2012). Circulating fluidized bed gasifiers can be operated at low temperatures (< 750 °C), which mitigates various ash sintering-derived problems such as fouling and corrosion (Ahrenfeldt et al., 2013; Shabangu et al., 2014; Thomsen et al., 2017). A low temperature circulating fluidized bed gasifier consisting of separate pyrolysis and gasification reactors has been developed to achieve a reaction temperature around 700 - 750 ^{o}C (Ahrenfeldt et al., 2013). The low reaction

temperature prevented the melting of ash compounds, and the gasifier is suitable for the gasification of feedstocks with high ash contents such as straw, manure, sewage sludge, and municipal solid waste.

2.2.3 Entrained flow

For entrained flow gasifiers (Fig. 2 (e)), the feedstock and gasifying agent are co-currently injected into the reactor from the top (Surisetty et al., 2012). The residence time is short in the order of a few to tens of seconds, which requires high temperature (> 1400 °C) and pulverized fine feedstock particles (< 0.1 - 0.4 mm) to achieve efficient carbon conversion (McKendry, 2002; Zhao et al., 2009). The high temperature effectively removes most of the tars but also leads to a low biochar yield (Öhrman et al., 2014). A carbon conversion efficiency of 95 - 99% was achieved in the existing large-scale systems (Promes et al., 2015). Ash is discharged as a molten slag containing a significant amount of metals.

Fibrous biomass such as wood is not suitable for this type of gasifier because: (1) additional effort and energy are needed to pulverize the feedstock and (2) the bulky density and high cohesive forces of the feedstock may lead to the issue of inconsistent feeding (Hu et al., 2012; Saber et al., 2016; Zwart et al., 2006). Typically, 10 - 20 kW energy was required to pulverize torrefied wood to a particle size of 100 μm at room temperature (Prins et al., 2006). Milling wood to 100 μm particles consumes around 0.08 kW_e/kW_{th} wood, while torrefaction pre-treatment can reduce the electricity consumption to 0.01-0.02 kW_e/kW_{th} wood (Van der Drift et al., 2004). Fine particles can be mixed with water to form a slurry to facilitate the feeding, and the added water serves as a reactant to promote H_2 production (Arena, 2012; Ruiz et al., 2013). Svoboda et al. (2009) proposed three methods for biomass feeding into pressurized entrained flow gasifiers: (1) wood torrefaction and grinding to a particle size < 0.2 mm followed by the existing feeding methods for dry, pulverized coals, (2) biomass-oil biochar

slurry (biochar content between 10 and 25 wt.%) preparation followed by pumping, and (3) wood or torrefied wood slurry preparation with waste glycerol or ethylene glycol followed by pumping. These methods served to minimize the overall energy loss and achieve relatively smooth biomass feeding into pressurized entrained flow gasifiers.

Considering the relatively high reactivity of woody biomass, Van der Drift et al. (2004) also suggested that woody biomass particles as large as 1 mm was suitable for entrained flow gasification, which saved the torrefaction pretreatment and made screw feeder suffice. Entrained flow gasifiers are normally used in large scale applications (> 50 MW), especially for integrated gasification combined cycle plants (Lee et al., 2014; Promes et al., 2015). Biomass can also be co-gasified with coal in entrained flow gasifiers. For example, co-gasification of 30% biomass with coal has been conducted in Nuon Buggenum plant (250 MWe) in the Netherlands (Simmons, 2011). Thattai et al. (2016) demonstrated that up to 70% (energy based) biomass can be mixed with coal for co-gasification in an existing 253 MW_e integrated gasification combined cycle power plants, which suggested a strong possibility of low emission/carbon neutral power plants. A feature comparison of different types of gasifiers is summarized in Table 1.

3 CONTAMINATION ISSUES

Various inorganic and organic contaminants such as ammonia (NH_3), hydrogen sulfide (H_2S), and tars are produced during the gasification process (Belgiorno et al., 2003; Torres et al., 2007). These contaminants potentially affect the post-stream applications of syngas and cause a series of problems such as conversion efficiency reduction, pipeline clogging, catalyst deactivation, pollutant emission, *etc* (Aravind & de Jong, 2012; Shen et al., 2015a). Hence, gas cleaning and conditioning costs amount to a significant part of the total expenses for the implementation of gasification systems.

Recently, increasing attention has been paid to biochar contamination, which is a particular concern for the biochar generated from wastes such as demolition wood waste, sewage sludge, industrial waste, diary manure, plastics waste, *etc* (Kim et al., 2015; Oleszczuk et al., 2013). These wastes contain various pollutants such as PAHs, dioxins, heavy metals, perfluorooctanoic acid (PFOA)/perfluorooctanesulfonic acid (PFOS), and polychlorinated biphenyls (PCBs) depending on specific industrial processes involved by the waste. Some of these pollutants (*e.g.*, PAHs and PCBs) are not fully decomposed and are even the products of the gasification process (Werle, 2015a). Most of the heavy metals were retained in gasification biochars with higher concentrations in smaller biochar particles due to vaporization and re-condensation of metal salts (Nzihou & Stanmore, 2013). The presence of contaminants adversely affects the environmental and economic sustainability of biochar applications.

3.1.1 Ammonia

Ammonia (NH_3) was related to the nitrogen content of feedstock (*e.g.*, coal and biomass). The NH_3 concentration in syngas was in the range of 0.06 - 0.4 % (Burch & Southward, 1999; Norton & Brown, 2005). Approximately 60 - 80 wt.% organic nitrogen is converted to NH_3 during gasification (Wang et al., 1999). It is noted that NH_3 serves as a NO_x precursor and hinders the conversion of H_2 and CO into liquid transportation fuels by poisoning the catalysts in the Fischer-Tropsch synthesis (Pansare & Goodwin Jr, 2008). The presence of NH_3 also interferes the syngas fermentation process that is widely used to upgrade syngas to value-added biofuels and chemicals. It rapidly converts to NH_4^+ upon its contact with fermentation media and the accumulation of NH_4^+ inhibited hydrogenase activity and cell growth, which reduces the carbon conversion efficiency and biofuel production of the fermentation process (Xu & Lewis, 2012).

Traditionally, NH_3 can be removed using a water scrubber or a flue gas condenser due to its water solubility. However, this method incurred extra operating costs because the product gas needs to be cooled down and NH_3 in the process water still needs to go through further treatment (Tunå & Brandin, 2013). A variety of catalysts (*e.g.*, Ni-, Ru-, Fe-, and W-based) have been developed to decompose NH_3 to H_2 and N_2 (Pansare & Goodwin Jr, 2008; Pansare et al., 2007). The NH_3 decomposing activity is restrained because of sulfur poisoning of nickel catalysts, and it was recommended that the catalyst process should operate at > 900°C to mitigate the sulfur poisoning effect at high pressure (2 - 3 MPa) (Hepola & Simell, 1997). Selective catalytic reduction was also applied and NH_3 was selectively oxidized with injected NO_X over a catalyst ($V_2O_5/WO_3/TiO_2$ or H-mordenite) (Tunå & Brandin, 2013). Over 90% NH_3 conversion was achieved under a NH_3:NO_2 stoichiometry of 1:1.25 when the temperature was 300 - 377 °C and 300 - 422 °C for $V_2O_5/WO_3/TiO_2$ and H-mordenite catalysts, respectively.

3.1.2 Hydrogen sulfide

Hydrogen sulfide (H_2S) has been found to be one of the major sulfur forms in product gas and its concentration can be up to 3 vol.% (Karmakar et al., 2015). The presence of H_2S corrodes piping components and deactivate catalysts, especially those used for syngas upgrading (Pinto et al., 2014; Roller et al., 2016). Hydrogen sulfide formation was associated with the presence of both sulfur and hydrogen in the feedstocks of entrained flow gasification, that is, high sulfur and hydrogen concentrations in feedstocks were needed for a large amount H_2S formation (Krishnamoorthy & Pisupati, 2016). The increase in O_2/C molar ratio during the circulating fluidized bed gasification of low rank coal was found to favor the transformation of H_2S to more stable forms (Zhang et al., 2016). Typical H_2S removal methods prior to catalytic syngas treatments are based on the reactions between H_2S and sulfur sorbents (metal oxides (*e.g.*, ZnO, CuO, CaO, *etc*)) (Meng et al., 2010; Yazdanbakhsh et al., 2016). *In situ*

desulfurization that introduces single metal oxides into a gasifier is economical and simple, but the sorbents need to be thermally and mechanically stable to maintain the thermodynamics of desulfurization under the condition of high temperature and friction (Husmann et al., 2014). Under high-temperature *in situ* desulfurization, reduction to elemental metal and metal evaporation occur for some metal oxides such as ZnO, CuO, MnO, and Fe_2O_3, lowering the sorbent reactivity and H_2S removal efficiency.

To improve the stability of metal oxides for sulfur sorption, the single sorbent material is combined to form mixed-metal oxides that can effectively mitigate the reduction and sulfate formation (Abbasian & Slimane, 1998). Zn-based mixed-metal sorbents showed orderly crystalline orientation and enlarged micro-pores without changes in particle sizes after 17-cycle tests (Bu et al., 2008). The mixed-metal oxide sorbents (Cu, Mo, and/or Mn metal oxides supported on a high silica-containing zeolite) were found to be able to retain their reactivity and crush strength during series of 5.5-cycle tests (Gasper-Galvin et al., 1998). Commonly used metal oxides-based sorbents cannot reduce the H_2S concentration below 100 ppm_v. Novel BaO-based sorbents that consisted of a mixed solution of 10% BaO and 90% CaO (*i.e.*, CaBa sorbent) have been developed to achieve desulfurization of below 1 ppm_v H_2S in a fixed-bed gasifier application (Stemmler et al., 2013). Husmann et al. (2014) explored the performance of the BaO-based sorbent in a bubbling fluidized bed gasifier and found that the CaBa sorbent achieved an *in situ* desulfurization down to 35 ppm_v H_2S with full conversion of BaO to BaS. But lime had to be added as a separating agent to prevent sintering of the CaBa sorbent and maintain stable gasification conditions in the gasifier. To enhance the adsorptive capacity of the sorbents, high surface area materials such as Al_2O_3, TiO_2, and zeolites were often used to support the metal oxides by increasing surface areas and cation exchange capacity (Rezaei et al., 2015; Yazdanbakhsh et al., 2014).

3.1.3 Tar

Tar is a complex mixture of condensable hydrocarbons and is generally referred to as all the organic contaminants (*e.g.*, aromatic organic compounds, oxygenated hydrocarbons, and PAHs) that have a molecular weight larger than benzene (Anis & Zainal, 2011). Based on the method of Milne et al. (1998), tar is classified into primary, secondary, and tertiary tar depending on the reaction temperature and compositions. The primary tars including furfural, acetates, and methoxyphenols were derived from the condensable volatile species released during the low thermal pyrolysis stage (400 – 700 ^{o}C). Under an elevated temperature of 700 – 850 ^{o}C, some part of primary tar is decomposed into small gaseous molecules under the effect of gasifying agent, while the rest of primary tar is transformed into secondary tars such as olefins and phenolics. The transformation of primary tar into secondary tar is most commonly achieved by the processes like dehydration, decarboxylation, and decarbonylation where small gaseous molecules are eliminated (Wolfesberger et al., 2009). Under a temperature of 850 – 1000 ^{o}C, primary tar is completely destroyed, and tertiary tar such as toluene, pyrene, and naphthalene is formed. Increasing temperature generally leads to an increase in the content of tertiary tar for gasification at atmospheric pressure (Rabou et al., 2009). For pressurized gasification, however, naphthalene decreases significantly with increasing temperature (Mayerhofer et al., 2012). Naphthalene is one of most stable tar components and has been commonly used as the surrogated molecule for tar reforming studies (Coll et al., 2001; Nestler et al., 2016). The formation of primary and secondary tar is favored by high heating rates, while low heating rates facilitate tertiary tar formation (Chen et al., 2009; Wei et al., 2006).

The liquefaction of condensable tars after cool-down blocks and corrodes piping components, and affect the energy efficiency of the overall process. Some tar components (*e.g.*, dichloromethane and PAHs) are toxicants that can cause headache, dizziness, nausea, and even cancer (Simell et al., 2000), therefore tar residues in biochar may pose potential health risks

during the application of biochar. PAHs condense onto gasification biochar when the biochar stays in contact with the tar-containing product gas at low temperatures (Hansen et al., 2015). Nuclear magnetic resonance spectroscopy demonstrated that tar was trapped in gasification biochar under pressurized environments, which may decrease the specific surface area of biochar and compromise their performance (Melligan et al., 2011).

The tar content in the product gas ranged from 50 to 500 mg/m^3, or can be up to 200 g/kg feedstock for fixed bed gasifiers (Bhattacharya & Pham, 2001; Kumar et al., 2010), in clear contrast to the permissible concentrations of < 100 mg/m^3 for internal combustion engines and < 1 mg/m^3 for industrial gas turbines (Hasler & Nussbaumer, 1999; Mastellone & Arena, 2008). The total content of 9 PAHs detected in the gasification biochar of wheat straw and wood chips were 5 and 0.69 mg kg^{-1}, respectively (Hansen et al., 2015). The concentrations of 16 priority PAHs in gasification biochar of various feedstocks (*e.g.*, conifer, poplar wood, wheat straw, sorghum, olive residue, and rice husk) ranged from less than 4 to 104 mg kg^{-1} (Shackley et al., 2012; Wiedner et al., 2013). Naphthalene accounted for approximately 40 - 60 wt. % of the PAHs on gasification biochar and it was the dominant PAH component among the 16 priority PAHs (Rollinson, 2016).

The dominant factors controlling tar production were throughput (*i.e.*, the mass of feedstock fed to a gasifier per unit time and per square meter of the cross-sectional area of gasifier), temperature, and type and dosage of catalysts (Rabou et al., 2009; Roche et al., 2014). High reaction temperatures in a gasifier promote the decomposition of tars via thermal cracking. For example, the amount of low molecular weight PAHs and aliphatic hydrocarbons produced in a downdraft gasifier decreased as temperature increased (Abioye & Ani, 2015). de Andrés et al. (2016) showed that increasing the temperature from 750 to 850 °C reduced the gravimetric tar production by 65% and 49% at the throughput of 110 and 322 kg/(h m^2), respectively, for fluidized bed gasification of sewage sludge. Gasification biochar from pine wood pellets had a

lower PAHs content than both fast and slow pyrolysis biochars (Yargicoglu et al., 2015). The relatively high temperature during the gasification process favored the decomposition of PAHs into smaller organic species (Botero et al., 2016). Using O_2 as the gasifying agent in the gasification process promotes the combustion of organic matter to CO_2 and thus mitigate the formation of PAHs (Spokas et al., 2011). However, the formation of CO_2 reduces the lower heating value of gasification product gas. Catalytic cracking involves the use of common catalysts such as nickel-based catalysts, alkali metal catalysts, acid catalysts, activated carbon catalysts, *etc* (Han & Kim, 2008). However, these commercial catalysts were easily deactivated by carbon fouling (*e.g.*, coke deposition on nickel-based catalysts) and contaminants in the product gas (Chan & Tanksale, 2014).

Low cost, high activity, resistance to degradation, and ease of regeneration are some of the key criteria in defining an effective catalyst for tar removal (Mani et al., 2013). The tar removal was found to be positively correlated with the surface area, pore diameter and pore volume of catalysts, and the temperature of reaction (Bhandari et al., 2014). Low cost gasification biochar are recently employed as catalysts to decompose tar. The tar removal efficiency of biochar and biochar-derived activated carbon was comparable with those of commercial catalysts such as transition metal-based catalysts (Świerczyński et al., 2007).

4 PRODUCT UPGRADING

4.1 Syngas upgrading

Syngas can be upgraded into value-added biofuel and chemicals (*e.g.*, ethanol, acetate, formate, butanol, *etc*) via either catalytic conversion or anaerobic fermentation (Xiong et al., 2017). Commonly used catalysts include copper-based catalysts, noble metal catalysts (*e.g.*, Rh and Pd), modified Fischer-Tropsch catalysts, and Mo-based catalysts (Spivey & Egbebi, 2007). Copper-based catalysts achieve relatively high selectivity and activity in the

temperature and pressure ranges of 280 - 310 °C and 4 - 10 MPa, and a low H_2/CO ratio (≤ 2) favored the selectivity toward higher alcohols (Gupta et al., 2011). Noble metal catalysts exhibit high activity in the temperature range of 250 - 350 °C, but their prohibitive costs make them economically unviable in many cases (Alijani & Irankhah, 2013). Refractory metal Mo-based catalysts were used in the temperature and pressure ranges of 200 - 320 °C and 1.6 - 9.7 MPa, with an alcohol selectivity of 25 - 27% (Yang & Ge, 2016a). Fe or Ni-based Fischer-Tropsch catalysts are typically modified by other promoters such as Cu and Co and are named modified Fischer-Tropsch catalysts receive an increasing attention due to their similar catalytic effect to the highly ethanol-selective Rh-based catalysts but much lower cost (Smith et al., 2012). Catalytic conversion is sensitive to syngas contaminants and has specific requirements to the H_2/CO ratio. For example, increasing the H_2/CO ratio from 1 to 3 enhanced the CO conversion by 20% and reduced dimethyl ether (DME) selectivity during the direct synthesis of DME from syngas using hybrid bifunctional catalysts consisting of Cu, Zn, and Mg materials and varying amounts of MgO (Asthana et al., 2016). In contrast, syngas fermentation via anaerobic microorganisms has a relatively high tolerance to contaminants such as H_2S and is less sensitive to the composition of syngas (Brown, 2007).

Anaerobic microorganisms (*carboxydotrophic homoacetogens*) can ferment syngas to produce biofuels and chemicals via the reductive acetyl-CoA pathway, where syngas is converted into acetyl-CoA that can be incorporated into biomass, and indirectly (via acetate) and directly reduced to acetaldehyde and then ethanol (Martin et al., 2016). The major challenges of syngas fermentation include the slow mass transfer of syngas components in fermentation medium and relatively low volumetric productivity (Drzyzga et al., 2015; Yang & Ge, 2016b). Stirred tank reactors and biotrickling filters (packed-bed reactor) have been developed to promote the mass transfer by increasing the specific surface area between syngas compositions and fermentation medium (Munasinghe & Khanal, 2010; Shen et al., 2017).

Membrane biofilm reactors (MBfR) where a biofilm is directly attached to the membrane through which the gases diffuse have been applied for syngas fermentation (Henstra et al., 2007). Typical advantages of MBfR include high gas utilization efficiencies, low energy consumption, and small reactor footprints. However, more research is warranted regarding biofilm management, and the design of scalable reactor and cost-effective membranes (Martin & Nerenberg, 2012), which are still challenging in large-scale applications.

Hydrogen production by promoting the WGS reaction (Eq. (6)) is a special type of syngas upgrading. Advancement in fuel cell technologies and increasing demand for renewable energy stimulate extensive research to produce environmentally friendly H_2 by upgrading the biomass-derived syngas featured by renewability and availability (Haryanto et al., 2009). The ratio between the H_2 energy content and biomass energy content was 83 corresponding to a H_2 yield of 11.5 wt.% for a gasification and shift reaction combined process (Balat & Kırtay, 2010). Traditionally, the WGS after a gasifier is carried out by a high-temperature (350 - 400 °C), Fe-Cr-catalyst-based stage, followed by a low-temperature (220 - 300 °C), Cu-Zn-catalyst-based shift with H_2 being purified in a subsequent separation stage (Brunetti et al., 2012). However, the Fe-Cr-based catalysts pose potential environmental and safety issues due to the presence of Cr compounds, while the Cu-Zn-based catalysts tend to undergo sintering and are susceptible to poisoning (Maroño et al., 2008). The presence of H_2 in syngas limits CO conversion thermodynamically (Eg. (5)) (Brunetti et al., 2009). The thermodynamic limits of syngas upgrading in a secondary reactor downstream was analyzed based on the minimization of Gibbs free energy function, and it was found that a temperature range of 630 - 730 °C led to a maximum H_2 yield and negligible CH_4 and coke formation (Haryanto et al., 2009). With this temperature range, H_2 increased by 43 - 124%, while CO_2 and CH_4 decreased by 24 - 64% and 100%, respectively. Huang et al. (2012) experimentally showed that the condensable products

in syngas can also be effectively upgraded to hydrogen in a secondary catalytic reactor with 7Ni-2Cu/Al_2O_3 under a mild temperature (250 °C).

Noble metal catalysts exhibit excellent performance in catalyzing the WGS reaction. For example, Haryanto et al. (2007) compared the performance of noble metals (Rh, Pt, Pd, Ir, Ru, and Ag) and Ni catalysts supported on CeO_2/Al_2O_3 at high temperatures (*i.e.*, 300, 500, and 700 °C), and found that Pt/CeO_2/Al_2O_3 and Ru/CeO_2/Al_2O_3 were the best catalysts in terms of activity as well as H_2 yield and selectivity. The authors suggested that these two catalysts were suitable for biomass gasification in a downstream reactor. Chein et al. (2014) showed that Pt/CeO_2/Al_2O_3 catalysts exhibited good thermal stability in the temperature range of 750 - 850 °C and bimetallic Pt-Ni/CeO_2/Al_2O_3 catalysts led to higher CO conversion compared to monometallic catalysts (Pt/Al_2O_3 or Pt/CeO_2/Al_2O_3). Maroño et al. (2008) showed that the CO concentration at the reactor outlet was reduced to less than 3% using a Pt/CeO_2/ZrO_2 catalyst in the temperature range of 300 - 400 °C, and CO conversion decreased as the space velocity increased or the H_2O/CO ratio decreased.

The WGS reaction and H_2 separation can be achieved simultaneously using membrane reactors, which shift the reaction toward further conversion by constantly removing the reaction product H_2 (Brunetti et al., 2012). The Pd-based membrane reactors have received an intensive attention due to their ability in separating and recovering a pure hydrogen stream with an ideal H_2 selectivity (100%). Brunetti et al. (2009) upgraded syngas for pure H_2 production using a membrane reactor with a Pd-Ag membrane and found that a CO conversion of *ca.* 90% was achieved compared to less than 22% in a traditional reactor. The produced H_2 stream was suitable for a proton-exchange membrane fuel cell. Brunetti et al. (2012) found that CO conversion in a membrane reactor with a Fe/Cr-based catalyst was two to three times higher than the equilibrium conversion in a traditional first stage (high temperature) reactor with the same catalyst. At 450 °C and 1 MPa, more than 90% of H_2 was recovered in the permeate as a

pure stream without requiring any further purification, suggesting that the two-reaction and one purification stage in the traditional process can be reduced to only one unit via a membrane reactor without compromising CO conversion.

The high cost is one of the major barriers to the scale-up application of Pd-based membranes. In recent, thin Pd-alloy supported membranes have been developed to improve the economic viability of syngas-derived H_2 (Gallucci et al., 2013). Brunetti et al. (2015) tested the performance of an ultra-thin (3.6 μm) Pd-Ag membrane for H_2 production, which achieved CO conversion of 96% and H_2 recovery of 84% at 2500 h^{-1}, 400 °C, and 0.4 MPa. Alternatively, low cost membranes such as porous silica membranes have also been adopted to catalyze the WGS reaction (Battersby et al., 2008; Wei & Kawamoto, 2013). However, water can potentially reduce the selectivity of Co-doped silica membranes by adsorbing on the surface of silica membrane and thus blocking micropores (Battersby et al., 2008). In general, porous silica membrane reactors achieved higher CO conversion than packed-bed reactors with the same catalysts (Brunetti et al., 2007; Wei & Kawamoto, 2013).

The WGS reaction can also be catalyzed by thermophilic microorganisms such as *Carboxydothermus hydrogenoformans* for H_2 production, which has the advantages of relatively high yields and cost efficiency over the catalyst-based WGS (Mohammadi et al., 2011). *C. hydrogenoformans* have been used in a hollow fiber membrane bioreactor (HFMBR) for syngas upgrading at a temperature of 70 °C and a relatively constant H_2 yield of 92 ± 4% (mol mol^{-1}) was achieved regardless of the operating conditions (Zhao et al., 2013b). However, the CO conversion in the HFMBR was bio-kinetically limited and the highest CO conversion activity was only 15% of the maximal potential of the strain under non-limiting conditions, due to the low dissolubility of CO (0.01 - 0.07 mM) in HFMBR liquid. The permeability of the membrane decreased over time due to membrane fouling and aging, which made the membrane unsuitable for long-term and high CO feeding application. Haddad et al. (2014) investigated

the *C. hydrogenoformans*-based microbial process in a gas-lift bioreactor where the medium was constantly agitated by a gas stream from a sparkler to improve the mass transfer of CO in the medium. The resulting H_2 yields were 95% and 82% ($mol_{H_2} \cdot mol_{CO}^{-1}$) with and without a growth support by peptone, and due to the low cell density, the volumetric activity in the gas-lift bioreactor was approximately 18 times lower than that in a biofilm-based system as studied by Zhao et al. (2013b).

Syngas upgrading plays a critical role in ensuring the practicality of gasification systems. Optimal upgrading approaches should be featured by reliability, security, affordability, and sustainability. Reliability means a great tolerance to syngas contaminants and robustness to syngas composition variation. Security suggests that the approaches can be easily operated, controlled, adjusted and maintained, and pose a negligible threat to the environment. The approaches should also be economically viable upon large-scale, practical deployment. This suggests that (1) the raw upgrading materials and systems should be low-cost and (2) the upgrading efficiency should be sufficiently high. Most of the existing approaches were tested by lab-scale experiments and thus barely suffered from the economic limitation as imposed during practical, large-scale applications. The approaches incorporating syngas contaminant removal with syngas upgrading can potentially achieve both reliability and affordability. The economic impact of syngas upgrading processes should be considered in the cost-benefit analysis of gasification systems. Sustainability means that the approaches should have a small carbon footprint by using renewable sources and they do not significantly increase the overall carbon footprint across the life cycle of syngas. Environmental sustainability can also be considered as an external cost in the cost-benefit analysis based on the monetary valuation of damages caused by the emissions during a process (Dincer & Acar, 2015). None of the existing methods contain all the features which should shape the directions of syngas upgrading design in the future.

4.2 Biochar upgrading/conversion

Thermal treatment can modify biochar's surface chemical properties as illustrated by existing studies on the surface modification of activated carbon (Abioye & Ani, 2015; Qi et al., 2017). Thermal treatment was generally conducted at high temperatures (700 - 1000 °C) and under H_2 or inert atmosphere, selectively removing some surface acidic functional groups (Figueiredo et al., 1999; Rajapaksha et al., 2016). Compared to an inert (*e.g.*, N_2) environment, H_2 environment was more effective to remove oxygen functional groups and deactivate active sites, thus making the carbon materials more stable (Shafeeyan et al., 2010). Thermal treatment based on microwave heating can result in a gradual decrease in surface acidic groups and increase in basic groups (Liu et al., 2010; Zhang et al., 2013). Compared to conventional heating, microwave heating offers obvious advantages such as fast, simple, inexpensive, and volumetric heating, homogeneous nucleating, and energy efficient (Abioye & Ani, 2015). Studies on microwave assisted pyrolysis suggest that microwave heating can potentially cause hotspots in the material being heated due to the nonuniform distribution of electromagnetic field and heterogeneous composition distribution (*i.e.*, thermo-electromagnetic properties) in the material (Luo et al., 2017; Luque et al., 2012; Mushtaq et al., 2016). The formation of hot spots is affected by the material position in the microwave field, the convection and radiation heat loss from the material, and the heterogeneity of dielectric properties throughout the material (Gadkari et al., 2017). In microwave assisted pyrolysis, the hotspot effect can serve to accelerate chemical reactions due to a thermal catalytic effect (Sun et al., 2012). Dai et al., (2017) showed that bamboo sawdust after microwave hydrothermal treatment had a higher HHV than that after conventional treatment the hotspot effect by microwave irradiation facilitated the breakage of C – H and C – O bonds and removed more acetyl groups.

Gasification biochar can be directly upgraded into oxygenated catalysts (Yuan et al., 2017b). The gasification biochar from poplar wood was oxygenated using O_2 treatment at temperatures ranging from 280 °C to 400 °C for 2 - 16 h to increase the oxygen content by chemisorption (Ducousso et al., 2015). During the process, the porosity and specific surface area were increased via moderate combustion, which compensated the surface area reduction induced by chemisorption. At a mid-range temperature, however, the oxygen atoms react with carbon matrix and induce an unintended mass loss. On the surface of the raw gasification biochar, the dominant functional groups were ether, quinone, phenol, and pyrone with percentages of 20%, 17%, 16%, and 14%, respectively. After the oxygenation treatment, there were increases in hydroxyl, peroxides, and lactones, and the formation of anhydrides, at the expense of reduction in quinone and pyrone, while ether and phenol remained at high percentages of 18%. Although the amount of total acidic groups increased after the oxygenation, the relatively strong acidic group (carboxylic acid) was reduced by 25%. The oxygenated biochar catalyst can be utilized as electrode materials, for the reduction of aromatic compounds, removal of SO_x and NO_x from flue gases, and dehydration/dehydrogenation of aliphatic alcohols (Fujita et al., 2014; Liu et al., 2012b; Seredych et al., 2008).

The recalcitrant carbon of gasification biochar is difficult to be consumed by microbes, whereas chemical and biological depolymerization transform biochar to less recalcitrant compounds. The chemical treatment involved the application of $KMnO_4$, H_2O_2, H_2SO_4, NaOH, ammonium peroxydisulfate, *etc* (Elmouwahidi et al., 2012; Jin et al., 2013; Liu et al., 2012a). For example, chemical agents ($KMnO_4$, H_2SO_4, and NaOH) have been used to depolymerize the gasification biochar of cotton waste and $KMnO_4$ showed the highest depolymerization capacity followed by NaOH and H_2SO_4 (Plácido & Capareda, 2015). The gasification biochar was transformed into profitable products such as silica and fulvic acids via the chemical depolymerization.

Microorganisms were also used in depolymerizing biochars, *i.e.*, biodepolymerization. The gasification biochar of cotton stalk was depolymerized using four fungal strains *Phanerochaete chrysosporium*, *Ceriporiopsis subvermispora*, *Postia placenta*, and *Bjerkandera adusta* for deploymerizing, of which *C. subvermispora* showed the largest depolymerization ability (Placido et al., 2016). The production of laccase and manganese peroxidase (MnP) was proposed to be one of the factors involved in the biodepolymerization of biochar. Laccases were associated with the catalysis of phenolic aromatics while MnP was associated with the cleavage of aromatic structures. A large amount of aromatic groups on biochar may favor the production and catalysis of laccase. Biochar contaminants such as PAHs and heavy metals, however, may inhibit the growth and enzymatic production of fungal strains during biodepolymerization, especially for the case of *P. chrysosporium* (Placido et al., 2016).

Gasification biochar has various application possibilities such as catalysts for tar removal and biodiesel production, gasification fuel, additives for anaerobic digestion, and electrochemical materials (You et al. (2017a) and references therein). These applications are closely associated with the physiochemical properties of biochar. It is important to modify the physiochemical properties of biochar and design corresponding upgrading approaches based on specific application requirements. For example, high carbon-oxygen groups in biochar favors its application as the carbon material in direct carbon fuel cells (DCFCs) (Elleuch et al., 2015), which can be facilitated by biochar oxygenation. Hence, biochar upgrading serves as an integral part of biochar application. Like the case of syngas upgrading, future research should aim to develop biochar upgrading approaches of reliability, security, affordability, and sustainability. Biochar upgrading and application can be combined with syngas upgrading to develop integrated syngas and biochar production and utilization systems. For example, the tar removal and adsorption ability of biochar make it a potential material for decontaminating product gas prior to its upgrading. An integrated perspective based on both life cycle

environmental assessment and economic analysis is needed to demystify the application potential of a combined production of syngas and biochar from gasification systems.

5 TECHNOLOGY POTENTIAL AND FUTURE DIRECTIONS

In the face of population expansion and rapid economy growth, there are worldwide concerns over soaring energy and resource demands, municipal solid waste pileup, and climate change. Among a variety of renewable technologies (*e.g.*, solar, wind, geothermal, and gasification), the prominent advantage of gasification is its ability to tackle these three concerns simultaneously, if waste biomass is used as the feedstock of the process. While the utilization of gasification main product (syngas) is relatively mature, increasing number of studies have shown the environmental and energy applications of gasification biochar (You et al., 2017a). Shabangu et al. (2014) studied the economic feasibility of co-production of methanol and biochar based on the gasification or pyrolysis of pine. They found that pyrolysis was not competitive based on methanol price alone without valorizing biochar, and the benefit from biochar selling accounted for about 10% of the total revenue for the gasification-based system. Most part of waste can be converted into valuable products via gasification and thus gasification-based waste disposal serves as a promoter towards zero waste and circular economy. Furthermore, due to the high stability of carbon in gasification biochar especially upon its soil application, it can serve as an effective carbon sequestration tool. There are quadruple benefits from a gasification system with biochar applied to soils: long-term carbon sequestration, renewable energy production, soil amendment, and waste management (Roberts et al., 2009). Roberts et al. (2009) showed that this kind of system achieved negative net greenhouse gas (GHG) emissions of -864 and -885 kg CO_2 equivalent per ton dry feedstock stover and yard waste, and 62 - 66% of this carbon mitigation was accounted for by carbon sequestration. In other words, from a life-cycle perspective, the carbon sequestration ability of

biochar significantly increased the carbon abatement potential of a gasification system, on top of the usual carbon emission savings by the displacement of fossil fuel use (You et al., 2017b). Considering that bioenergy makes up approximately 77% of world's renewable energy (Atewamba and Boimah, 2017), the gasification-based energy production is expected to play a major role in future energy supply and climate change mitigation.

However, technological barriers are still a roadblock to a wide implementation of gasification and indicate the future directions of gasification research and development. First, slagging and agglomeration-related issues exist across almost all types of gasifiers and adversely affect the stability of gasification. Existing gasification models and simulation (*e.g.*, (Adeyemi & Janajreh, 2015; Jeong et al., 2014; Yan et al., 2018; Yao et al., 2018)) can hardly capture or predict the instability, which suggests great uncertainty about modeling and simulating actual gasification processes. It is important to systematically understand the fundamental mechanisms underlying the issues, and relevant models covering the slagging and agglomeration are essential for accurately designing gasification systems. Meanwhile, it is also necessary to develop specific mitigation measures for different types of gasifiers.

Second, contamination deteriorates the quality of gasification products and thus the economic benefits of gasification systems. Countermeasures are available, but their economic feasibility and large-scale application still need to be tested. For example, catalysts such as nickel and noble metal-based ones add a significant cost component to a gasification system, and the effectiveness of the large-scale application of the catalysts remains a question. Hence, it is highly desirable to develop cost-effective decontamination measures and test their techno-economic feasibility upon large-scale applications which is still lacking. One of the potential solutions is to re-utilize the gasification co-products directly for the decontamination and upgrading (*e.g.*, combining biochar upgrading and application with syngas upgrading), and form a product use closed-loop inside the system (Wang et al., 2014). Biochar-derived catalysts

have been developed to decompose tar, which provides a promising means for lowering the cost of decontamination (Bhandari et al., 2014; Mani et al., 2013). Nanocatalysts can also be used to reduce the overall cost of catalyst use because they allow expensive catalytic elements to be dispersed onto high surface area supports (Kathiraser et al., 2016).

Third, the physiochemical properties of syngas and biochar are closely associated with the operating conditions of gasification which determine the performance of product application. Towards accurate and flexible designing and optimization of gasification systems, *e.g.*, in terms of life cycle assessment (LCA) and cost-benefit analysis (CBA), the functional relationships among the operating conditions (*e.g.*, temperature, heating rate, gasifier configurations, feedstock types and properties, *etc*), the physiochemical properties (*e.g.*, composition and heating value of syngas, and specific surface area, fixed carbon content, pH of biochar, *etc*) of co-products, and application outcomes (*e.g.*, energy output, chemical efficiency and productivity, soil amendment effect, tar cracking effect, *etc*) need to be identified. For example, Field et al. (2013) proposed a mechanistic model for integrated LCA and CBA of a biochar and bioenergy coproduction system based on biomass residue feedstocks. They coupled thermochemical biomass conversion dataset with the mechanistic model of agronomic responses and modelled product yields and biochar recalcitrance as continuous functions of temperature.

Fourth, economic viability, carbon abatement potential, and waste volume reduction ability are the three major indicators upon gasification system design. Since different stakeholders (*e.g.*, policymakers, investors, and consumers) have different demands upon technology development, multiple indicators with different relative weightings need to be considered in decision support analysis for a comprehensive evaluation (Dong et al., 2014). Relevant optimization models are needed to identify the optimal system plans with the consideration of the integration of gasification with upstream and downstream components. Due to the vast

possibilities of technology and process alternatives, conventional methods such as total enumeration, evolutionary methods, and hierarchical decomposition methods are either computationally inefficient or do not guarantee optimal solutions. Superstructure optimization based on mixed-integer programming techniques enables systematic generation and automatic evaluation of design candidates with the best process economics and highest levels of environmental sustainability (Gong & You, 2015). Multi-objective optimization frameworks can be developed by integrating the techno-economic and life cycle sustainability analyses into the superstructure optimization (You et al., 2012). In this case, the identified optimal plans regarding population density, harvesting sites of biomass, biomass resource distribution, and consumer distribution serve as the basis for suggesting on the formulation of effective policy and subsidy incentives, and bioenergy action plans.

6 CONCLUSIONS

The reduction stage critically determines the syngas composition and productivity, and the compositions, surface morphology, fixed carbon aromaticity, and other chemical properties of biochars. Scale requirement (*e.g.*, volume of feedstock and energy demand), feedstock characteristics (*e.g.*, moisture and ash content), and the quality of syngas and biochar need to be considered upon the selection of gasifiers. Catalysts (*e.g.*, Ni-based) are available to decompose NH_3 to H_2 and N_2. Metal oxides (*e.g.*, ZnO, CuO, CaO, *etc*) were used as sorbents to remove H_2S prior to catalytic syngas treatment. The mixed metal oxides effectively mitigate the sulfate formation and improve the mechanical strength, structure, and reactivity of sorbents. High reaction temperature in a gasifier promotes the decomposition of tars via thermal cracking. Catalytic cracking of tars was closely related to the surface area, pore diameter and pore volume of catalysts, and the temperature of reaction. Catalytic conversion or anaerobic fermentation were used to upgrade syngas into value-added biofuel and chemicals. Thermal, chemical, and

biological treatments can be applied to modify the surface physiochemical properties of biochar for bespoke applications. Future syngas and biochar upgrading methods should be featured by reliability, security, affordability, and sustainability, towards the practical, large-scale production of syngas and biochar. One potential solution is to develop integrated systems by combining biochar upgrading and application with syngas upgrading, which warrants an integrated perspective based on both life cycle environmental assessment and economic analysis.

ACKNOWLEDGEMENT

Chi-Hwa Wang and Siming You acknowledge the funding support by the National Research Foundation (NRF), Prime Minister's Office, Singapore under its Campus for Research Excellence and Technological Enterprise (CREATE) program. Grant Number R-706-001-101-281, National University of Singapore.

REFERENCES

Abbasian, J., Slimane, R.B. 1998. A regenerable copper-based sorbent for H_2S removal from coal gases. *Industrial & Engineering Chemistry Research*, **37**(7), 2775-2782.

Abioye, A.M., Ani, F.N. 2015. Recent development in the production of activated carbon electrodes from agricultural waste biomass for supercapacitors: A review. *Renewable and Sustainable Energy Reviews*, **52**, 1282-1293.

Adeyemi, I., Janajreh, I. 2015. Modeling of the entrained flow gasification: Kinetics-based ASPEN Plus model. *Renewable Energy*, **82**, 77-84.

Ahrenfeldt, J., Thomsen, T.P., Henriksen, U., Clausen, L.R. 2013. Biomass gasification cogeneration–A review of state of the art technology and near future perspectives. *Applied Thermal Engineering*, **50**(2), 1407-1417.

Alijani, A., Irankhah, A. 2013. Medium‐Temperature Shift Catalysts for Hydrogen Purification in a Single-Stage Reactor. *Chemical Engineering & Technology*, **36**(2), 209-219.

Anca-Couce, A., Mehrabian, R., Scharler, R., Obernberger, I. 2014. Kinetic scheme of biomass pyrolysis considering secondary charring reactions. *Energy Conversion and Management*, **87**, 687-696.

Angın, D. 2013. Effect of pyrolysis temperature and heating rate on biochar obtained from pyrolysis of safflower seed press cake. *Bioresource Technology*, **128**, 593-597.

Anis, S., Zainal, Z. 2011. Tar reduction in biomass producer gas via mechanical, catalytic and thermal methods: A review. *Renewable and Sustainable Energy Reviews*, **15**(5), 2355-2377.

Aranda, G., Grootjes, A., Van der Meijden, C., Van der Drift, A., Gupta, D., Sonde, R., Poojari, S., Mitra, C. 2016. Conversion of high-ash coal under steam and CO2 gasification conditions. *Fuel Processing Technology*, **141**, 16-30.

Aravind, P., de Jong, W. 2012. Evaluation of high temperature gas cleaning options for biomass gasification product gas for solid oxide fuel cells. *Progress in Energy and Combustion Science*, **38**(6), 737-764.

Arena, U. 2012. Process and technological aspects of municipal solid waste gasification. A review. *Waste Management*, **32**(4), 625-639.

Asadullah, M., Adi, A.M., Suhada, N., Malek, N.H., Saringat, M.I., Azdarpour, A. 2014. Optimization of palm kernel shell torrefaction to produce energy densified bio-coal. *Energy Conversion and Management*, **88**, 1086-1093.

Asthana, S., Samanta, C., Bhaumik, A., Banerjee, B., Voolapalli, R.K., Saha, B. 2016. Direct synthesis of dimethyl ether from syngas over Cu-based catalysts: Enhanced selectivity in the presence of MgO. *Journal of Catalysis*, **334**, 89-101.

Asthana, S., Samanta, C., Voolapalli, R.K., Saha, B. 2017. Direct conversion of syngas to DME: synthesis of new Cu-based hybrid catalysts using Fehling's solution, elimination of the calcination step. *Journal of Materials Chemistry A*, **5**(6), 2649-2663.

Aziz, M., Prawisudha, P., Prabowo, B., Budiman, B.A. 2015. Integration of energy-efficient empty fruit bunch drying with gasification/combined cycle systems. *Applied Energy*, **139**, 188-195.

Babu, B., Sheth, P.N. 2006. Modeling and simulation of reduction zone of downdraft biomass gasifier: effect of char reactivity factor. *Energy Conversion and Management*, **47**(15), 2602-2611.

Balat, H., Kırtay, E. 2010. Hydrogen from biomass–present scenario and future prospects. *International Journal of Hydrogen Energy*, **35**(14), 7416-7426.

Balat, M., Balat, M., Kırtay, E., Balat, H. 2009. Main routes for the thermo-conversion of biomass into fuels and chemicals. Part 2: Gasification systems. *Energy Conversion and Management*, **50**(12), 3158-3168.

Barisano, D., Freda, C., Nanna, F., Fanelli, E., Villone, A. 2012. Biomass gasification and in-bed contaminants removal: Performance of iron enriched Olivine and bauxite in a process of steam/O_2 gasification. *Bioresource Technology*, **118**, 187-194.

Battersby, S., Duke, M.C., Liu, S., Rudolph, V., da Costa, J.C.D. 2008. Metal doped silica membrane reactor: operational effects of reaction and permeation for the water gas shift reaction. *Journal of Membrane Science*, **316**(1), 46-52.

Beenackers, A. 1999. Biomass gasification in moving beds, a review of European technologies. *Renewable Energy*, **16**(1-4), 1180-1186.

Belgiorno, V., De Feo, G., Della Rocca, C., Napoli, R. 2003. Energy from gasification of solid wastes. *Waste Management*, **23**(1), 1-15.

Bhandari, P.N., Kumar, A., Bellmer, D.D., Huhnke, R.L. 2014. Synthesis and evaluation of biochar-derived catalysts for removal of toluene (model tar) from biomass-generated producer gas. *Renewable Energy*, **66**, 346-353.

Bhattacharya, S., Pham, H.-L. 2001. A study on a multi-stage hybrid gasifier-engine system. *Biomass and Bioenergy*, **21**(6), 445-460.

Botero, M.L., Chen, D., González-Calera, S., Jefferson, D., Kraft, M. 2016. HRTEM evaluation of soot particles produced by the non-premixed combustion of liquid fuels. *Carbon*, **96**, 459-473.

Brar, J., Singh, K., Wang, J., Kumar, S. 2012. Cogasification of coal and biomass: A review. *International Journal of Forestry Research*, **2012**.

Brewer, C.E., Unger, R., Schmidt-Rohr, K., Brown, R.C. 2011. Criteria to select biochars for field studies based on biochar chemical properties. *BioEnergy Research*, **4**(4), 312-323.

Broer, K.M., Brown, R.C. 2015. Effect of equivalence ratio on partitioning of nitrogen during biomass gasification. *Energy & Fuels*, **30**(1), 407-413.

Brown, R.C. 2007. Hybrid thermochemical/biological processing. *Applied Biochemistry and Biotecnology*, 947-956.

Brunetti, A., Barbieri, G., Drioli, E. 2009. Pd-based membrane reactor for syngas upgrading. *Energy & Fuels*, **23**(10), 5073-5076.

Brunetti, A., Barbieri, G., Drioli, E., Lee, K.-H., Sea, B., Lee, D.-W. 2007. WGS reaction in a membrane reactor using a porous stainless steel supported silica membrane. *Chemical Engineering and Processing: Process Intensification*, **46**(2), 119-126.

Brunetti, A., Caravella, A., Drioli, E., Barbieri, G. 2012. Process intensification by membrane reactors: high-temperature water gas shift reaction as single stage for syngas upgrading. *Chemical Engineering & Technology*, **35**(7), 1238-1248.

Brunetti, A., Caravella, A., Fernandez, E., Tanaka, D.P., Gallucci, F., Drioli, E., Curcio, E., Viviente, J., Barbieri, G. 2015. Syngas upgrading in a membrane reactor with thin Pd-alloy supported membrane. *International Journal of Hydrogen Energy*, **40**(34), 10883-10893.

Bu, X., Ying, Y., Zhang, C., Peng, W. 2008. Research improvement in Zn-based sorbent for hot gas desulfurization. *Powder Technology*, **180**(1-2), 253-258.

Buragohain, B., Mahanta, P., Moholkar, V.S. 2010. Biomass gasification for decentralized power generation: The Indian perspective. *Renewable and Sustainable Energy Reviews*, **14**(1), 73-92.

Burch, R., Southward, B.W. 1999. Highly selective catalysts for conversion of ammonia to nitrogen in gasified biomass. *Chemical Communications*(16), 1475-1476.

Campoy, M., Gómez-Barea, A., Ollero, P., Nilsson, S. 2014. Gasification of wastes in a pilot fluidized bed gasifier. *Fuel Processing Technology*, **121**, 63-69.

Cetin, E., Gupta, R., Moghtaderi, B. 2005. Effect of pyrolysis pressure and heating rate on radiata pine char structure and apparent gasification reactivity. *Fuel*, **84**(10), 1328-1334.

Ceylan, S., Topçu, Y. 2014. Pyrolysis kinetics of hazelnut husk using thermogravimetric analysis. *Bioresource Technology*, **156**, 182-188.

Cha, J.S., Park, S.H., Jung, S.-C., Ryu, C., Jeon, J.-K., Shin, M.-C., Park, Y.-K. 2016. Production and utilization of biochar: A review. *Journal of Industrial and Engineering Chemistry*, **40**, 1-15.

Chan, F.L., Tanksale, A. 2014. Review of recent developments in Ni-based catalysts for biomass gasification. *Renewable and Sustainable Energy Reviews*, **38**, 428-438.

Chein, R., Lin, Y., Chen, Y., Chyou, Y., Chung, J. 2014. Study on water-gas shift reaction performance using Pt-based catalysts at high temperatures. *International Journal of Hydrogen Energy*, **39**(33), 18854-18862.

Chen, C., Jin, Y.-Q., Yan, J.-H., Chi, Y. 2013. Simulation of municipal solid waste gasification in two different types of fixed bed reactors. *Fuel*, **103**, 58-63.

Chen, D., Zhou, J., Zhang, Q. 2014. Effects of heating rate on slow pyrolysis behavior, kinetic parameters and products properties of moso bamboo. *Bioresource Technology*, **169**, 313-319.

Chen, G., Yao, J., Yang, H., Yan, B., Chen, H. 2015. Steam gasification of acid-hydrolysis biomass CAHR for clean syngas production. *Bioresource Technology*, **179**, 323-330.

Chen, S., Yang, R. 1997. Unified mechanism of alkali and alkaline earth catalyzed gasification reactions of carbon by CO2 and H2O. *Energy & Fuels*, **11**(2), 421-427.

Chen, Y., Luo, Y.-h., Wu, W.-g., Su, Y. 2009. Experimental investigation on tar formation and destruction in a lab-scale two-stage reactor. *Energy & Fuels*, **23**(9), 4659-4667.

Chhiti, Y., Kemiha, M. 2013. Thermal conversion of biomass, pyrolysis and gasification. *International Journal of Engineering and Science*, **2**(3), 75-85.

Chmielniak, T., Sciazko, M. 2003. Co-gasification of biomass and coal for methanol synthesis. *Applied Energy*, **74**(3), 393-403.

Cho, D.-W., Kwon, G., Ok, Y.S., Kwon, E.E., Song, H. 2017a. Reduction of Bromate by Cobalt-Impregnated Biochar Fabricated via Pyrolysis of Lignin Using CO2 as a Reaction Medium. *ACS Applied Materials & Interfaces*, **9**(15), 13142-13150.

Cho, D.-W., Kwon, G., Yoon, K., Tsang, Y.F., Ok, Y.S., Kwon, E.E., Song, H. 2017b. Simultaneous production of syngas and magnetic biochar via pyrolysis of paper mill sludge using CO 2 as reaction medium. *Energy Conversion and Management*, **145**, 1-9.

Ciferno, J.P., Marano, J.J. 2002. Benchmarking biomass gasification technologies for fuels, chemicals and hydrogen production. *US Department of Energy. National Energy Technology Laboratory*.

Coll, R., Salvado, J., Farriol, X., Montane, D. 2001. Steam reforming model compounds of biomass gasification tars: conversion at different operating conditions and tendency towards coke formation. *Fuel Processing Technology*, **74**(1), 19-31.

Craven, J., Swithenbank, J., Sharifi, V., Peralta-Solorio, D., Kelsall, G., Sage, P. 2014. Development of a novel solids feed system for high pressure gasification. *Fuel Processing Technology*, **119**, 32-40.

Dai, L., He, C., Wang, Y., Liu, Y., Yu, Z., Zhou, Y., Fan, L., Duan, D., Ruan, R. 2017. Comparative study on microwave and conventional hydrothermal pretreatment of bamboo sawdust: Hydrochar properties and its pyrolysis behaviors. *Energy Conversion and Management*, **146**, 1-7.

Das, B., Datta, A. 2016. Modeling of hydrodynamics in a bubbling fluidized-bed gasifier and evaluation of the inter-phase gas exchange rate under different operating conditions. *Particuology*, **25**, 151-158.

de Andrés, J.M., Roche, E., Narros, A., Rodríguez, M.E. 2016. Characterisation of tar from sewage sludge gasification. Influence of gasifying conditions: Temperature, throughput, steam and use of primary catalysts. *Fuel*, **180**, 116-126.

Demirbas, A. 2004. Effects of temperature and particle size on bio-char yield from pyrolysis of agricultural residues. *Journal of Analytical and Applied Pyrolysis*, **72**(2), 243-248.

Di Blasi, C. 2009. Combustion and gasification rates of lignocellulosic chars. *Progress in Energy and Combustion Science*, **35**(2), 121-140.

Di Blasi, C., Branca, C. 2013. Modeling a stratified downdraft wood gasifier with primary and secondary air entry. *Fuel*, **104**, 847-860.

Dincer, I., Acar, C. 2015. Review and evaluation of hydrogen production methods for better sustainability. *International Journal of Hydrogen Energy*, **40**(34), 11094-11111.

Dogru, M., Howarth, C., Akay, G., Keskinler, B., Malik, A. 2002. Gasification of hazelnut shells in a downdraft gasifier. *Energy*, **27**(5), 415-427.

Dong, J., Chi, Y., Zou, D., Fu, C., Huang, Q., Ni, M. 2014. Energy–environment–economy assessment of waste management systems from a life cycle perspective: Model development and case study. *Applied Energy*, **114**, 400-408.

Drzyzga, O., Revelles, O., Durante‐Rodríguez, G., Díaz, E., García, J.L., Prieto, A. 2015. New challenges for syngas fermentation: towards production of biopolymers. *Journal of Chemical Technology and Biotechnology*, **90**(10), 1735-1751.

Ducousso, M., Weiss-Hortala, E., Nzihou, A., Castaldi, M.J. 2015. Reactivity enhancement of gasification biochars for catalytic applications. *Fuel*, **159**, 491-499.

Elleuch, A., Halouani, K., Li, Y. 2015. Investigation of chemical and electrochemical reactions mechanisms in a direct carbon fuel cell using olive wood charcoal as sustainable fuel. *Journal of Power Sources*, **281**, 350-361.

Elmouwahidi, A., Zapata-Benabithe, Z., Carrasco-Marín, F., Moreno-Castilla, C. 2012. Activated carbons from KOH-activation of argan (Argania spinosa) seed shells as supercapacitor electrodes. *Bioresource Technology*, **111**, 185-190.

Erkiaga, A., Lopez, G., Amutio, M., Bilbao, J., Olazar, M. 2014. Influence of operating conditions on the steam gasification of biomass in a conical spouted bed reactor. *Chemical Engineering Journal*, **237**, 259-267.

Fagbemi, L., Khezami, L., Capart, R. 2001. Pyrolysis products from different biomasses: application to the thermal cracking of tar. *Applied Energy*, **69**(4), 293-306.

Fernandez-Lopez, M., Pedroche, J., Valverde, J., Sanchez-Silva, L. 2017. Simulation of the gasification of animal wastes in a dual gasifier using Aspen Plus®. *Energy Conversion and Management*, **140**, 211-217.

Ferreira, A.G., Maia, C.B., Cortez, M.F., Valle, R.M. 2008. Technical feasibility assessment of a solar chimney for food drying. *Solar Energy*, **82**(3), 198-205.

Field, J.L., Keske, C.M., Birch, G.L., DeFoort, M.W., Cotrufo, M.F. 2013. Distributed biochar and bioenergy coproduction: a regionally specific case study of environmental benefits and economic impacts. *Gcb Bioenergy*, **5**(2), 177-191.

Figueiredo, J., Pereira, M., Freitas, M., Orfao, J. 1999. Modification of the surface chemistry of activated carbons. *Carbon*, **37**(9), 1379-1389.

Fouilland, T., Grace, J.R., Ellis, N. 2010. Recent advances in fluidized bed technology in biomass processes. *Biofuels*, **1**(3), 409-433.

Fujita, S.-i., Watanabe, H., Katagiri, A., Yoshida, H., Arai, M. 2014. Nitrogen and oxygen-doped metal-free carbon catalysts for chemoselective transfer hydrogenation of nitrobenzene, styrene, and 3-nitrostyrene with hydrazine. *Journal of Molecular Catalysis A: Chemical*, **393**, 257-262.

Gadkari, S., Fidalgo, B., Gu, S. 2017. Numerical investigation of microwave-assisted pyrolysis of lignin. *Fuel Processing Technology*, **156**, 473-484.

Gai, C., Chen, M., Liu, T., Peng, N., Liu, Z. 2016. Gasification characteristics of hydrochar and pyrochar derived from sewage sludge. *Energy*, **113**, 957-965.

Gallucci, F., Fernandez, E., Corengia, P., van Sint Annaland, M. 2013. Recent advances on membranes and membrane reactors for hydrogen production. *Chemical Engineering Science*, **92**, 40-66.

Gasper-Galvin, L.D., Atimtay, A.T., Gupta, R.P. 1998. Zeolite-supported metal oxide sorbents for hot-gas desulfurization. *Industrial & Engineering Chemistry Research*, **37**(10), 4157-4166.

Gómez-Barea, A., Ollero, P., Leckner, B. 2013. Optimization of char and tar conversion in fluidized bed biomass gasifiers. *Fuel*, **103**, 42-52.

Gong, J., You, F. 2015. Sustainable design and synthesis of energy systems. *Current Opinion in Chemical Engineering*, **10**, 77-86.

Guangul, F.M., Sulaiman, S.A., Ramli, A. 2012. Gasifier selection, design and gasification of oil palm fronds with preheated and unheated gasifying air. *Bioresource Technology*, **126**, 224-232.

Guangul, F.M., Sulaiman, S.A., Ramli, A. 2014. Study of the effects of operating factors on the resulting producer gas of oil palm fronds gasification with a single throat downdraft gasifier. *Renewable Energy*, **72**, 271-283.

Gujar, A.C., Baik, J., Garceau, N., Muradov, N., Ali, T. 2014. Oxygen-blown gasification of pine charcoal in a top-lit downdraft moving-hearth gasifier. *Fuel*, **118**, 27-32.

Gül, S., Akgün, F., Aydar, E., Ünlü, N. 2018. Pressurized gasification of lignite in a pilot scale bubbling fluidized bed reactor with air, oxygen, steam and CO2 agents. *Applied Thermal Engineering*, **130**, 203-210.

Gupta, M., Smith, M.L., Spivey, J.J. 2011. Heterogeneous catalytic conversion of dry syngas to ethanol and higher alcohols on Cu-based catalysts. *Acs Catalysis*, **1**(6), 641-656.

Haddad, M., Cimpoia, R., Guiot, S.R. 2014. Performance of Carboxydothermus hydrogenoformans in a gas-lift reactor for syngas upgrading into hydrogen. *International Journal of Hydrogen Energy*, **39**(6), 2543-2548.

Han, J., Kim, H. 2008. The reduction and control technology of tar during biomass gasification/pyrolysis: An overview. *Renewable and Sustainable Energy Reviews*, **12**(2), 397-416.

Hansen, V., Müller-Stöver, D., Ahrenfeldt, J., Holm, J.K., Henriksen, U.B., Hauggaard-Nielsen, H. 2015. Gasification biochar as a valuable by-product for carbon sequestration and soil amendment. *Biomass and Bioenergy*, **72**, 300-308.

Haryanto, A., Fernando, S., Adhikari, S. 2007. Ultrahigh temperature water gas shift catalysts to increase hydrogen yield from biomass gasification. *Catalysis Today*, **129**(3), 269-274.

Haryanto, A., Fernando, S.D., Pordesimo, L.O., Adhikari, S. 2009. Upgrading of syngas derived from biomass gasification: A thermodynamic analysis. *Biomass and Bioenergy*, **33**(5), 882-889.

Hasler, P., Nussbaumer, T. 1999. Gas cleaning for IC engine applications from fixed bed biomass gasification. *Biomass and Bioenergy*, **16**(6), 385-395.

Haynes, W.M. 2014. *CRC handbook of chemistry and physics*. CRC press.

Henstra, A.M., Sipma, J., Rinzema, A., Stams, A.J. 2007. Microbiology of synthesis gas fermentation for biofuel production. *Current Opinion in Biotechnology*, **18**(3), 200-206.

Hepola, J., Simell, P. 1997. Sulphur poisoning of nickel-based hot gas cleaning catalysts in synthetic gasification gas: I. Effect of different process parameters. *Applied Catalysis B: Environmental*, **14**(3), 287-303.

Hernando, H., Jiménez-Sánchez, S., Fermoso, J., Pizarro, P., Coronado, J., Serrano, D. 2016. Assessing biomass catalytic pyrolysis in terms of deoxygenation pathways and energy yields for the efficient production of advanced biofuels. *Catalysis Science & Technology*, **6**(8), 2829-2843.

Hognon, C., Dupont, C., Grateau, M., Delrue, F. 2014. Comparison of steam gasification reactivity of algal and lignocellulosic biomass: influence of inorganic elements. *Bioresource Technology*, **164**, 347-353.

Hosseinpour, S., Aghbashlo, M., Tabatabaei, M., Younesi, H., Mehrpooya, M., Ramakrishna, S. 2017. Multi-objective exergy-based optimization of a continuous photobioreactor applied to produce hydrogen using a novel combination of soft computing techniques. *International Journal of Hydrogen Energy*, **42**(12), 8518-8529.

Hu, J., Yu, F., Lu, Y. 2012. Application of Fischer–Tropsch synthesis in biomass to liquid conversion. *Catalysts*, **2**(2), 303-326.

Huang, B.-S., Chen, H.-Y., Kuo, J.-H., Chang, C.-H., Wey, M.-Y. 2012. Catalytic upgrading of syngas from fluidized bed air gasification of sawdust. *Bioresource Technology*, **110**, 670-675.

Huang, C., Wu, X., Huang, Y., Lai, C., Li, X., Yong, Q. 2016. Prewashing enhances the liquid hot water pretreatment efficiency of waste wheat straw with high free ash content. *Bioresource Technology*, **219**, 583-588.

Huang, Z., Zhang, J., Zhao, Y., Zhang, H., Yue, G., Suda, T., Narukawa, M. 2010. Kinetic studies of char gasification by steam and CO 2 in the presence of H 2 and CO. *Fuel Processing Technology*, **91**(8), 843-847.

Husmann, M., Hochenauer, C., Meng, X., Jong, W.d., Kienberger, T. 2014. Evaluation of sorbents for high temperature in situ desulfurization of biomass-derived syngas. *Energy & Fuels*, **28**(4), 2523-2534.

Iliuta, I., Leclerc, A., Larachi, F. 2010. Allothermal steam gasification of biomass in cyclic multi-compartment bubbling fluidized-bed gasifier/combustor-New reactor concept. *Bioresource Technology*, **101**(9), 3194-3208.

Im-orb, K., Simasatitkul, L., Arpornwichanop, A. 2016. Analysis of synthesis gas production with a flexible H 2/CO ratio from rice straw gasification. *Fuel*, **164**, 361-373.

Inyang, M.I., Gao, B., Yao, Y., Xue, Y., Zimmerman, A., Mosa, A., Pullammanappallil, P., Ok, Y.S., Cao, X. 2016. A review of biochar as a low-cost adsorbent for aqueous heavy metal removal. *Critical Reviews in Environmental Science and Technology*, **46**(4), 406-433.

James R, A.M., Yuan, W., Boyette, M.D. 2016. The effect of biomass physical properties on top-lit updraft gasification of woodchips. *Energies*, **9**(4), 283.

Jeong, H.J., Seo, D.K., Hwang, J. 2014. CFD modeling for coal size effect on coal gasification in a two-stage commercial entrained-bed gasifier with an improved char gasification model. *Applied Energy*, **123**, 29-36.

Jiang, L., Hu, S., Wang, Y., Su, S., Sun, L., Xu, B., He, L., Xiang, J. 2015. Catalytic effects of inherent alkali and alkaline earth metallic species on steam gasification of biomass. *International Journal of Hydrogen Energy*, **40**(45), 15460-15469.

Jin, H., Wang, X., Gu, Z., Polin, J. 2013. Carbon materials from high ash biochar for supercapacitor and improvement of capacitance with HNO_3 surface oxidation. *Journal of Power Sources*, **236**, 285-292.

Kaewluan, S., Pipatmanomai, S. 2011. Gasification of high moisture rubber woodchip with rubber waste in a bubbling fluidized bed. *Fuel Processing Technology*, **92**(3), 671-677.

Karmakar, M.K., Chandra, P., Chatterjee, P.K. 2015. A review on the fuel gas cleaning technologies in gasification process. *Journal of Environmental Chemical Engineering*, **3**(2), 689-702.

Kathiraser, Y., Ashok, J., Kawi, S. 2016. Synthesis and evaluation of highly dispersed SBA-15 supported Ni–Fe bimetallic catalysts for steam reforming of biomass derived tar reaction. *Catalysis Science & Technology*, **6**(12), 4327-4336.

Kim, J.H., Ok, Y.S., Choi, G.-H., Park, B.-J. 2015. Residual perfluorochemicals in the biochar from sewage sludge. *Chemosphere*, **134**, 435-437.

Kim, K.H., Kim, J.-Y., Cho, T.-S., Choi, J.W. 2012. Influence of pyrolysis temperature on physicochemical properties of biochar obtained from the fast pyrolysis of pitch pine (Pinus rigida). *Bioresource Technology*, **118**, 158-162.

Kim, M., Lee, Y., Park, J., Ryu, C., Ohm, T.-I. 2016. Partial oxidation of sewage sludge briquettes in a updraft fixed bed. *Waste Management*, **49**, 204-211.

Klimantos, P., Koukouzas, N., Katsiadakis, A., Kakaras, E. 2009. Air-blown biomass gasification combined cycles (BGCC): System analysis and economic assessment. *Energy*, **34**(5), 708-714.

Krishnamoorthy, V., Pisupati, S.V. 2015. A critical review of mineral matter related issues during gasification of coal in fixed, fluidized, and entrained flow gasifiers. *Energies*, **8**(9), 10430-10463.

Krishnamoorthy, V., Pisupati, S.V. 2016. Fate of sulfur during entrained-flow gasification of Pittsburgh No. 8 Coal: influence of particle size, sulfur forms, and temperature. *Energy & Fuels*, **30**(4), 3241-3250.

Kumar, A., Demirel, Y., Jones, D.D., Hanna, M.A. 2010. Optimization and economic evaluation of industrial gas production and combined heat and power generation from gasification of corn stover and distillers grains. *Bioresource Technology*, **101**(10), 3696-3701.

Kumar, A., Jones, D.D., Hanna, M.A. 2009. Thermochemical biomass gasification: a review of the current status of the technology. *Energies*, **2**(3), 556-581.

Kumar, K.V., Bharath, M., Raghavan, V., Prasad, B., Chakravarthy, S., Sundararajan, T. 2017a. Gasification of high-ash Indian coal in bubbling fluidized bed using air and steam–An experimental study. *Applied Thermal Engineering*, **116**, 372-381.

Kumar, U., Maroufi, S., Rajarao, R., Mayyas, M., Mansuri, I., Joshi, R.K., Sahajwalla, V. 2017b. Cleaner production of iron by using waste macadamia biomass as a carbon resource. *Journal of Cleaner Production*, **158**, 218-224.

Lahijani, P., Zainal, Z.A., Mohamed, A.R., Mohammadi, M. 2013. Co-gasification of tire and biomass for enhancement of tire-char reactivity in CO_2 gasification process. *Bioresource Technology*, **138**, 124-130.

Lee, J., Lee, T., Ok, Y.S., Oh, J.-I., Kwon, E.E. 2017a. Using CO_2 to mitigate evolution of harmful chemical compounds during thermal degradation of printed circuit boards. *Journal of CO_2 Utilization*, **20**, 66-72.

Lee, J., Yang, X., Cho, S.-H., Kim, J.-K., Lee, S.S., Tsang, D.C., Ok, Y.S., Kwon, E.E. 2017b. Pyrolysis process of agricultural waste using CO 2 for waste management, energy recovery, and biochar fabrication. *Applied Energy*, **185**, 214-222.

Lee, J.C., Lee, H.H., Joo, Y.J., Lee, C.H., Oh, M. 2014. Process simulation and thermodynamic analysis of an IGCC (integrated gasification combined cycle) plant with an entrained coal gasifier. *Energy*, **64**, 58-68.

Lee, T., Lee, J., Ok, Y.S., Oh, J.-I., Lee, S.-R., Rinklebe, J., Kwon, E.E. 2017c. Utilizing CO 2 as an Effective Carbon Scavenger to Suppress the Generation of Harmful Chemicals from the Thermal Degradation of Polyvinyl Chloride. *Journal of Cleaner Production*.

Lee, Y., Park, J., Ryu, C., Gang, K.S., Yang, W., Park, Y.-K., Jung, J., Hyun, S. 2013a. Comparison of biochar properties from biomass residues produced by slow pyrolysis at 500 C. *Bioresource Technology*, **148**, 196-201.

Lee, Y., Ryu, C., Park, Y.-K., Jung, J.-H., Hyun, S. 2013b. Characteristics of biochar produced from slow pyrolysis of Geodae-Uksae 1. *Bioresource Technology*, **130**, 345-350.

Li, C.-Z. 2007. Some recent advances in the understanding of the pyrolysis and gasification behaviour of Victorian brown coal. *Fuel*, **86**(12), 1664-1683.

Li, C.-Z., Sathe, C., Kershaw, J., Pang, Y. 2000. Fates and roles of alkali and alkaline earth metals during the pyrolysis of a Victorian brown coal. *Fuel*, **79**(3-4), 427-438.

Li, D., Briens, C., Berruti, F. 2015. Improved lignin pyrolysis for phenolics production in a bubbling bed reactor-effect of bed materials. *Bioresource Technology*, **189**, 7-14.

Liu, H., Kaneko, M., Kato, S., Kojima, T. 2003. Gasification of seven coals in carbon dioxide at elevated temperatures and high heating rates: Unification approach of reactivity. *Journal of Chemical Engineering of Japan*, **36**(7), 751-758.

Liu, M.-C., Kong, L.-B., Zhang, P., Luo, Y.-C., Kang, L. 2012a. Porous wood carbon monolith for high-performance supercapacitors. *Electrochimica Acta*, **60**, 443-448.

Liu, P., Liu, W.-J., Jiang, H., Chen, J.-J., Li, W.-W., Yu, H.-Q. 2012b. Modification of bio-char derived from fast pyrolysis of biomass and its application in removal of tetracycline from aqueous solution. *Bioresource Technology*, **121**, 235-240.

Liu, Q.-S., Zheng, T., Li, N., Wang, P., Abulikemu, G. 2010. Modification of bamboo-based activated carbon using microwave radiation and its effects on the adsorption of methylene blue. *Applied Surface Science*, **256**(10), 3309-3315.

Liu, Y., Aziz, M., Kansha, Y., Tsutsumi, A. 2013. A novel exergy recuperative drying module and its application for energy-saving drying with superheated steam. *Chemical Engineering Science*, **100**, 392-401.

Loha, C., Gu, S., De Wilde, J., Mahanta, P., Chatterjee, P.K. 2014. Advances in mathematical modeling of fluidized bed gasification. *Renewable and Sustainable Energy Reviews*, **40**, 688-715.

Lu, Y., Jin, H., Guo, L., Zhang, X., Cao, C., Guo, X. 2008. Hydrogen production by biomass gasification in supercritical water with a fluidized bed reactor. *International Journal of Hydrogen Energy*, **33**(21), 6066-6075.

Luo, H., Bao, L., Kong, L., Sun, Y. 2017. Low temperature microwave-assisted pyrolysis of wood sawdust for phenolic rich compounds: Kinetics and dielectric properties analysis. *Bioresource Technology*, **238**, 109-115.

Luque, R., Menendez, J.A., Arenillas, A., Cot, J. 2012. Microwave-assisted pyrolysis of biomass feedstocks: the way forward? *Energy & Environmental Science*, **5**(2), 5481-5488.

Lythcke-Jørgensen, C., Clausen, L.R., Algren, L., Hansen, A.B., Münster, M., Gadsbøll, R.Ø., Haglind, F. 2017. Optimization of a flexible multi-generation system based on wood chip gasification and methanol production. *Applied Energy*, **192**, 337-359.

Mandl, C., Obernberger, I., Scharler, I. 2011. Characterisation of fuel bound nitrogen in the gasification process and the staged combustion of producer gas from the updraft gasification of softwood pellets. *Biomass and Bioenergy*, **35**(11), 4595-4604.

Mani, S., Kastner, J.R., Juneja, A. 2013. Catalytic decomposition of toluene using a biomass derived catalyst. *Fuel Processing Technology*, **114**, 118-125.

Manyà, J.J. 2012. Pyrolysis for biochar purposes: a review to establish current knowledge gaps and research needs. *Environmental Science & Technology*, **46**(15), 7939-7954.

Manyà, J.J., Ruiz, J., Arauzo, J. 2007. Some peculiarities of conventional pyrolysis of several agricultural residues in a packed bed reactor. *Industrial & Engineering Chemistry Research*, **46**(26), 9061-9070.

Maroño, M., Sánchez, J., Ruiz, E., Cabanillas, A. 2008. Study of the suitability of a Pt-based catalyst for the upgrading of a biomass gasification syngas stream via the WGS reaction. *Catalysis Letters*, **126**(3-4), 396-406.

Martin, K.J., Nerenberg, R. 2012. The membrane biofilm reactor (MBfR) for water and wastewater treatment: principles, applications, and recent developments. *Bioresource Technology*, **122**, 83-94.

Martin, M.E., Richter, H., Saha, S., Angenent, L.T. 2016. Traits of selected Clostridium strains for syngas fermentation to ethanol. *Biotechnology and Bioengineering*, **113**(3), 531-539.

Mastellone, M.L., Arena, U. 2008. Olivine as a tar removal catalyst during fluidized bed gasification of plastic waste. *AIChE Journal*, **54**(6), 1656-1667.

Maya, D.M.Y., Sarmiento, A.L.E., de Sales, C.A.V.B., Oliveira, E.E.S.L., Andrade, R. 2016. Gasification of municipal solid waste for power generation in brazil, a review of available

technologies and their environmental benefits. *Journal of Chemistry and Chemical Engineering*, **10**, 249-255.

Mayerhofer, M., Mitsakis, P., Meng, X., de Jong, W., Spliethoff, H., Gaderer, M. 2012. Influence of pressure, temperature and steam on tar and gas in allothermal fluidized bed gasification. *Fuel*, **99**, 204-209.

McKendry, P. 2002. Energy production from biomass (part 3): gasification technologies. *Bioresource Technology*, **83**(1), 55-63.

Melligan, F., Auccaise, R., Novotny, E., Leahy, J., Hayes, M., Kwapinski, W. 2011. Pressurised pyrolysis of Miscanthus using a fixed bed reactor. *Bioresource Technology*, **102**(3), 3466-3470.

Meng, X., De Jong, W., Pal, R., Verkooijen, A.H. 2010. In bed and downstream hot gas desulphurization during solid fuel gasification: A review. *Fuel Processing Technology*, **91**(8), 964-981.

Milne, T.A., Evans, R.J., Abatzaglou, N. 1998. Biomass gasifier"Tars": their nature, formation, and conversion. National Renewable Energy Laboratory, Golden, CO (US).

Mohammadi, M., Najafpour, G.D., Younesi, H., Lahijani, P., Uzir, M.H., Mohamed, A.R. 2011. Bioconversion of synthesis gas to second generation biofuels: A review. *Renewable and Sustainable Energy Reviews*, **15**(9), 4255-4273.

Mohan, D., Sarswat, A., Ok, Y.S., Pittman, C.U. 2014. Organic and inorganic contaminants removal from water with biochar, a renewable, low cost and sustainable adsorbent–a critical review. *Bioresource Technology*, **160**, 191-202.

Moneti, M., Di Carlo, A., Bocci, E., Foscolo, P., Villarini, M., Carlini, M. 2016. Influence of the main gasifier parameters on a real system for hydrogen production from biomass. *International Journal of Hydrogen Energy*, **41**(28), 11965-11973.

Munasinghe, P.C., Khanal, S.K. 2010. Biomass-derived syngas fermentation into biofuels: Opportunities and challenges. *Bioresource Technology*, **101**(13), 5013-5022.

Muroyama, A.P., Loutzenhiser, P.G. 2016. Kinetic Analyses of Gasification and Combustion Reactions of Carbonaceous Feedstocks for a Hybrid Solar/Autothermal Gasification Process To Continuously Produce Synthesis Gas. *Energy & Fuels*, **30**(5), 4292-4299.

Murthy, M.R. 2009. A review of new technologies, models and experimental investigations of solar driers. *Renewable and Sustainable Energy Reviews*, **13**(4), 835-844.

Mushtaq, F., Mat, R., Ani, F.N. 2016. Fuel production from microwave assisted pyrolysis of coal with carbon surfaces. *Energy Conversion and Management*, **110**, 142-153.

Nestler, F., Burhenne, L., Amtenbrink, M.J., Aicher, T. 2016. Catalytic decomposition of biomass tars: The impact of wood char surface characteristics on the catalytic performance for naphthalene removal. *Fuel Processing Technology*, **145**, 31-41.

Newalkar, G., Iisa, K., D'Amico, A.D., Sievers, C., Agrawal, P. 2014. Effect of temperature, pressure, and residence time on pyrolysis of pine in an entrained flow reactor. *Energy & Fuels*, **28**(8), 5144-5157.

Nilsson, S., Gómez-Barea, A., Ollero, P. 2013. Gasification of char from dried sewage sludge in fluidized bed: Reaction rate in mixtures of CO2 and H2O. *Fuel*, **105**, 764-768.

Norton, G.A., Brown, R.C. 2005. Wet chemical method for determining levels of ammonia in syngas from a biomass gasifier. *Energy & Fuels*, **19**(2), 618-624.

Nzihou, A., Stanmore, B. 2013. The fate of heavy metals during combustion and gasification of contaminated biomass-A brief review. *Journal of Hazardous Materials*, **256**, 56-66.

Oh, J.-I., Lee, J., Lee, T., Ok, Y.S., Lee, S.-R., Kwon, E.E. 2017. Strategic CO_2 utilization for shifting carbon distribution from pyrolytic oil to syngas in pyrolysis of food waste. *Journal of CO_2 Utilization*, **20**, 150-155.

Öhrman, O.G., Molinder, R., Weiland, F., Johansson, A.C. 2014. Analysis of trace compounds generated by pressurized oxygen blown entrained flow biomass gasification. *Environmental Progress & Sustainable Energy*, **33**(3), 699-705.

Oleszczuk, P., Jośko, I., Kuśmierz, M. 2013. Biochar properties regarding to contaminants content and ecotoxicological assessment. *Journal of Hazardous Materials*, **260**, 375-382.

Ollero, P., Serrera, A., Arjona, R., Alcantarilla, S. 2003. The CO_2 gasification kinetics of olive residue. *Biomass and Bioenergy*, **24**(2), 151-161.

Ong, Z., Cheng, Y., Maneerung, T., Yao, Z., Tong, Y.W., Wang, C.H., Dai, Y. 2015. Co-gasification of woody biomass and sewage sludge in a fixed-bed downdraft gasifier. *AIChE Journal*, **61**(8), 2508-2521.

Pansare, S.S., Goodwin Jr, J.G. 2008. Ammonia decomposition on tungsten-based catalysts in the absence and presence of syngas. *Industrial & Engineering Chemistry Research*, **47**(12), 4063-4070.

Pansare, S.S., Torres, W., Goodwin, J.G. 2007. Ammonia decomposition on tungsten carbide. *Catalysis Communications*, **8**(4), 649-654.

Papari, S., Hawboldt, K. 2015. A review on the pyrolysis of woody biomass to bio-oil: Focus on kinetic models. *Renewable and Sustainable Energy Reviews*, **52**, 1580-1595.

Park, J., Lee, Y., Ryu, C., Park, Y.-K. 2014. Slow pyrolysis of rice straw: analysis of products properties, carbon and energy yields. *Bioresource Technology*, **155**, 63-70.

Parthasarathy, P., Narayanan, K.S. 2014. Hydrogen production from steam gasification of biomass: influence of process parameters on hydrogen yield–a review. *Renewable Energy*, **66**, 570-579.

Patel, M., Zhang, X., Kumar, A. 2016. Techno-economic and life cycle assessment on lignocellulosic biomass thermochemical conversion technologies: A review. *Renewable and Sustainable Energy Reviews*, **53**, 1486-1499.

Patil, K., Bhoi, P., Huhnke, R., Bellmer, D. 2011. Biomass downdraft gasifier with internal cyclonic combustion chamber: Design, construction, and experimental results. *Bioresource Technology*, **102**(10), 6286-6290.

Patra, T.K., Sheth, P.N. 2015. Biomass gasification models for downdraft gasifier: A state-of-the-art review. *Renewable and Sustainable Energy Reviews*, **50**, 583-593.

Pfeifer, C., Koppatz, S., Hofbauer, H. 2011. Steam gasification of various feedstocks at a dual fluidised bed gasifier: Impacts of operation conditions and bed materials. *Biomass Conversion and Biorefinery*, **1**(1), 39-53.

Pfeifer, C., Rauch, R., Hofbauer, H. 2004. In-bed catalytic tar reduction in a dual fluidized bed biomass steam gasifier. *Industrial & Engineering Chemistry Research*, **43**(7), 1634-1640.

Pinto, F., André, R.N., Carolino, C., Miranda, M. 2014. Hot treatment and upgrading of syngas obtained by co-gasification of coal and wastes. *Fuel Processing Technology*, **126**, 19-29.

Plácido, J., Capareda, S. 2015. Production of silicon compounds and fulvic acids from cotton wastes biochar using chemical depolymerization. *Industrial Crops and Products*, **67**, 270-280.

Placido, J., Capareda, S., Karthikeyan, R. 2016. Production of humic substances from cotton stalks biochar by fungal treatment with Ceriporiopsis subvermispora. *Sustainable Energy Technologies and Assessments*, **13**, 31-37.

Pode, R. 2016. Potential applications of rice husk ash waste from rice husk biomass power plant. *Renewable and Sustainable Energy Reviews*, **53**, 1468-1485.

Prins, M.J., Ptasinski, K.J., Janssen, F.J. 2007. From coal to biomass gasification: Comparison of thermodynamic efficiency. *Energy*, **32**(7), 1248-1259.

Prins, M.J., Ptasinski, K.J., Janssen, F.J. 2006. More efficient biomass gasification via torrefaction. *Energy*, **31**(15), 3458-3470.

Priyadarsan, S., Annamalai, K., Sweeten, J., Mukhtar, S., Holtzapple, M. 2004. Fixed-bed gasification of feedlot manure and poultry litter biomass. *Transactions of American Society of Agricultural and Biological Engineers*, **47**(5), 1689-1696.

Promes, E., Woudstra, T., Schoenmakers, L., Oldenbroek, V., Thattai, A.T., Aravind, P. 2015. Thermodynamic evaluation and experimental validation of 253MW integrated coal gasification combined cycle power plant in Buggenum, Netherlands. *Applied Energy*, **155**, 181-194.

Puig-Arnavat, M., Bruno, J.C., Coronas, A. 2010. Review and analysis of biomass gasification models. *Renewable and Sustainable Energy Reviews*, **14**(9), 2841-2851.

Qi, F., Kuppusamy, S., Naidu, R., Bolan, N.S., Ok, Y.S., Lamb, D., Li, Y., Yu, L., Semple, K.T., Wang, H. 2017. Pyrogenic Carbon and Its Role in Contaminant Immobilization in Soils. *Critical Reviews in Environmental Science and Technology*(just-accepted), 00-00.

Quyn, D.M., Wu, H., Li, C.-Z. 2002. Volatilisation and catalytic effects of alkali and alkaline earth metallic species during the pyrolysis and gasification of Victorian brown coal. Part I. Volatilisation of Na and Cl from a set of NaCl-loaded samples. *Fuel*, **81**(2), 143-149.

Rabou, L.P., Zwart, R.W., Vreugdenhil, B.J., Bos, L. 2009. Tar in biomass producer gas, the Energy research Centre of the Netherlands (ECN) experience: an enduring challenge. *Energy & Fuels*, **23**(12), 6189-6198.

Rajapaksha, A.U., Chen, S.S., Tsang, D.C., Zhang, M., Vithanage, M., Mandal, S., Gao, B., Bolan, N.S., Ok, Y.S. 2016. Engineered/designer biochar for contaminant removal/immobilization from soil and water: potential and implication of biochar modification. *Chemosphere*, **148**(27), 6e291.

Rapagnà, S., Gallucci, K., Di Marcello, M., Matt, M., Nacken, M., Heidenreich, S., Foscolo, P.U. 2010. Gas cleaning, gas conditioning and tar abatement by means of a catalytic filter candle in a biomass fluidized-bed gasifier. *Bioresource Technology*, **101**(18), 7123-7130.

Rezaei, H., Lim, C.J., Lau, A., Bi, X., Sokhansanj, S. 2016. Development of Empirical Drying Correlations for Ground Wood Chip and Ground Wood Pellet Particles. *Drying Technology*(just-accepted).

Rezaei, S., Jarligo, M.O.D., Wu, L., Kuznicki, S.M. 2015. Breakthrough performances of metal-exchanged nanotitanate ETS-2 adsorbents for room temperature desulfurization. *Chemical Engineering Science*, **123**, 444-449.

Roberts, K.G., Gloy, B.A., Joseph, S., Scott, N.R., Lehmann, J. 2009. Life cycle assessment of biochar systems: estimating the energetic, economic, and climate change potential. *Environmental Science & Technology*, **44**(2), 827-833.

Roche, E., de Andrés, J.M., Narros, A., Rodríguez, M.E. 2014. Air and air-steam gasification of sewage sludge. The influence of dolomite and throughput in tar production and composition. *Fuel*, **115**, 54-61.

Roller, D., Bläsing, M., Dreger, I., Yazdanbakhsh, F., Sawada, J.A., Kuznicki, S.M., Müller, M. 2016. Removal of hydrogen sulfide by metal-doped nanotitanate under gasification-like conditions. *Industrial & Engineering Chemistry Research*, **55**(14), 3871-3878.

Rollinson, A.N. 2016. Gasification reactor engineering approach to understanding the formation of biochar properties. *Proceedings of the Royal Society A: Mathematical, Physical & Engineering Sciences*. The Royal Society. pp. 20150841.

Ronsse, F., Van Hecke, S., Dickinson, D., Prins, W. 2013. Production and characterization of slow pyrolysis biochar: influence of feedstock type and pyrolysis conditions. *Gcb Bioenergy*, **5**(2), 104-115.

Ruiz, J., Juárez, M., Morales, M., Muñoz, P., Mendívil, M. 2013. Biomass gasification for electricity generation: review of current technology barriers. *Renewable and Sustainable Energy Reviews*, **18**, 174-183.

Ryu, C., Yang, Y.B., Khor, A., Yates, N.E., Sharifi, V.N., Swithenbank, J. 2006. Effect of fuel properties on biomass combustion: part I. Experiments-fuel type, equivalence ratio and particle size. *Fuel*, **85**(7), 1039-1046.

Saber, A.H., Göktepe, B., Umeki, K., Lundström, T.S., Gebart, R. 2016. Active fuel particles dispersion by synthetic jet in an entrained flow gasifier of biomass: Cold flow. *Powder Technology*, **302**, 275-282.

Sanchez-Silva, L., López-González, D., Villaseñor, J., Sánchez, P., Valverde, J. 2012. Thermogravimetric-mass spectrometric analysis of lignocellulosic and marine biomass pyrolysis. *Bioresource Technology*, **109**, 163-172.

Seredych, M., Hulicova-Jurcakova, D., Lu, G.Q., Bandosz, T.J. 2008. Surface functional groups of carbons and the effects of their chemical character, density and accessibility to ions on electrochemical performance. *Carbon*, **46**(11), 1475-1488.

Shabangu, S., Woolf, D., Fisher, E.M., Angenent, L.T., Lehmann, J. 2014. Techno-economic assessment of biomass slow pyrolysis into different biochar and methanol concepts. *Fuel*, **117**, 742-748.

Shabbir, I., Mirzaeian, M. 2016. Feasibility analysis of different cogeneration systems for a paper mill to improve its energy efficiency. *International Journal of Hydrogen Energy*, **41**(37), 16535-16548.

Shackley, S., Carter, S., Knowles, T., Middelink, E., Haefele, S., Sohi, S., Cross, A., Haszeldine, S. 2012. Sustainable gasification-biochar systems? A case-study of rice-husk gasification in Cambodia, Part I: Context, chemical properties, environmental and health and safety issues. *Energy Policy*, **42**, 49-58.

Shafeeyan, M.S., Daud, W.M.A.W., Houshmand, A., Shamiri, A. 2010. A review on surface modification of activated carbon for carbon dioxide adsorption. *Journal of Analytical and Applied Pyrolysis*, **89**(2), 143-151.

Sharma, A., Pareek, V., Zhang, D. 2015. Biomass pyrolysis—a review of modelling, process parameters and catalytic studies. *Renewable and Sustainable Energy Reviews,* **50**, 1081-1096.

Shen, Y., Brown, R.C., Wen, Z. 2017. Syngas fermentation by Clostridium carboxidivorans P7 in a horizontal rotating packed bed biofilm reactor with enhanced ethanol production. *Applied Energy*, **187**, 585-594.

Shen, Y., Chen, M., Sun, T., Jia, J. 2015a. Catalytic reforming of pyrolysis tar over metallic nickel nanoparticles embedded in pyrochar. *Fuel*, **159**, 570-579.

Shen, Y., Zhao, P., Shao, Q., Takahashi, F., Yoshikawa, K. 2015b. In situ catalytic conversion of tar using rice husk char/ash supported nickel–iron catalysts for biomass pyrolytic gasification combined with the mixing-simulation in fluidized-bed gasifier. *Applied Energy*, **160**, 808-819.

Sheth, P.N., Babu, B. 2009. Experimental studies on producer gas generation from wood waste in a downdraft biomass gasifier. *Bioresource Technology*, **100**(12), 3127-3133.

Simell, P., Ståhlberg, P., Kurkela, E., Albrecht, J., Deutsch, S., Sjöström, K. 2000. Provisional protocol for the sampling and anlaysis of tar and particulates in the gas from large-scale biomass gasifiers. Version 1998. *Biomass and Bioenergy*, **18**(1), 19-38.

Simmons, B.A. 2011. *Chemical and Biochemical Catalysis for Next Generation Biofuels*. Royal Society of Chemistry.

Simone, M., Nicolella, C., Tognotti, L. 2013. Numerical and experimental investigation of downdraft gasification of woody residues. *Bioresource Technology*, **133**, 92-101.

Smith, M.L., Kumar, N., Spivey, J.J. 2012. CO adsorption behavior of Cu/SiO_2, Co/SiO_2, and $CuCo/SiO_2$ catalysts studied by in situ DRIFTS. *Journal of Physical Chemistry C*, **116**(14), 7931-7939.

Spivey, J.J., Egbebi, A. 2007. Heterogeneous catalytic synthesis of ethanol from biomass-derived syngas. *Chemical Society Reviews*, **36**(9), 1514-1528.

Spokas, K.A., Novak, J.M., Stewart, C.E., Cantrell, K.B., Uchimiya, M., DuSaire, M.G., Ro, K.S. 2011. Qualitative analysis of volatile organic compounds on biochar. *Chemosphere*, **85**(5), 869-882.

Stark, A.K., Altantzis, C., Bates, R.B., Ghoniem, A.F. 2016. Towards an advanced reactor network modeling framework for fluidized bed biomass gasification: Incorporating information from detailed CFD simulations. *Chemical Engineering Journal*, **303**, 409-424.

Stemmler, M., Tamburro, A., Müller, M. 2013. Laboratory investigations on chemical hot gas cleaning of inorganic trace elements for the "UNIQUE" process. *Fuel*, **108**, 31-36.

Suliman, W., Harsh, J.B., Abu-Lail, N.I., Fortuna, A.-M., Dallmeyer, I., Garcia-Perez, M. 2016. Influence of feedstock source and pyrolysis temperature on biochar bulk and surface properties. *Biomass and Bioenergy*, **84**, 37-48.

Sun, J., Wang, W., Liu, Z., Ma, Q., Zhao, C., Ma, C. 2012. Kinetic study of the pyrolysis of waste printed circuit boards subject to conventional and microwave heating. *Energies*, **5**(9), 3295-3306.

Sun, Y., Gao, B., Yao, Y., Fang, J., Zhang, M., Zhou, Y., Chen, H., Yang, L. 2014. Effects of feedstock type, production method, and pyrolysis temperature on biochar and hydrochar properties. *Chemical Engineering Journal*, **240**, 574-578.

Surisetty, V.R., Kozinski, J., Dalai, A.K. 2012. Biomass, availability in Canada, and gasification: An overview. *Biomass Conversion and Biorefinery*, **2**(1), 73-85.

Svoboda, K., Pohořelý, M., Hartman, M., Martinec, J. 2009. Pretreatment and feeding of biomass for pressurized entrained flow gasification. *Fuel Processing Technology*, **90**(5), 629-635.

Sweeney, D.J. 2012. *Performance of a pilot-scale, steam-blown, pressurized fluidized bed biomass gasifier*. The University of Utah.

Świerczyński, D., Libs, S., Courson, C., Kiennemann, A. 2007. Steam reforming of tar from a biomass gasification process over Ni/olivine catalyst using toluene as a model compound. *Applied Catalysis B: Environmental*, **74**(3), 211-222.

Taba, L.E., Irfan, M.F., Daud, W.A.M.W., Chakrabarti, M.H. 2012. The effect of temperature on various parameters in coal, biomass and CO-gasification: A review. *Renewable and Sustainable Energy Reviews*, **16**(8), 5584-5596.

Tanner, J., Kabir, K.B., Müller, M., Bhattacharya, S. 2015. Low temperature entrained flow pyrolysis and gasification of a Victorian brown coal. *Fuel*, **154**, 107-113.

Tay, H.-L., Kajitani, S., Zhang, S., Li, C.-Z. 2013. Effects of gasifying agent on the evolution of char structure during the gasification of Victorian brown coal. *Fuel*, **103**, 22-28.

Thattai, A.T., Oldenbroek, V., Schoenmakers, L., Woudstra, T., Aravind, P. 2016. Experimental model validation and thermodynamic assessment on high percentage (up to 70%) biomass co-gasification at the 253 MWe integrated gasification combined cycle power plant in Buggenum, The Netherlands. *Applied Energy*, **168**, 381-393.

Thomsen, T.P., Sárossy, Z., Gøbel, B., Stoholm, P., Ahrenfeldt, J., Frandsen, F.J., Henriksen, U.B. 2017. Low temperature circulating fluidized bed gasification and co-gasification of municipal sewage sludge. Part 1: Process performance and gas product characterization. *Waste Management*.

Tinaut, F.V., Melgar, A., Perez, J.F., Horrillo, A. 2008. Effect of biomass particle size and air superficial velocity on the gasification process in a downdraft fixed bed gasifier. An experimental and modelling study. *Fuel Processing Technology*, **89**(11), 1076-1089.

Torres, W., Pansare, S.S., Goodwin Jr, J.G. 2007. Hot gas removal of tars, ammonia, and hydrogen sulfide from biomass gasification gas. *Catalysis Reviews*, **49**(4), 407-456.

Tremel, A., Haselsteiner, T., Kunze, C., Spliethoff, H. 2012a. Experimental investigation of high temperature and high pressure coal gasification. *Applied Energy*, **92**, 279-285.

Tremel, A., Haselsteiner, T., Nakonz, M., Spliethoff, H. 2012b. Coal and char properties in high temperature entrained flow gasification. *Energy*, **45**(1), 176-182.

Tunå, P., Brandin, J. 2013. Selective catalytic oxidation of ammonia by nitrogen oxides in a model synthesis gas. *Fuel*, **105**, 331-337.

Udomsirichakorn, J., Salam, P.A. 2014. Review of hydrogen-enriched gas production from steam gasification of biomass: the prospect of CaO-based chemical looping gasification. *Renewable and Sustainable Energy Reviews*, **30**, 565-579.

Van der Drift, A., Boerrigter, H., Coda, B., Cieplik, M., Hemmes, K., Van Ree, R., Veringa, H. 2004. Entrained flow gasification of biomass. *Energy Centre of Netherlands*.

Vera, D., Jurado, F., Carpio, J., Kamel, S. 2018. Biomass gasification coupled to an EFGT-ORC combined system to maximize the electrical energy generation: A case applied to the olive oil industry. *Energy*, **144**, 41-53.

Vriesman, P., Heginuz, E., Sjöström, K. 2000. Biomass gasification in a laboratory-scale AFBG: influence of the location of the feeding point on the fuel-N conversion. *Fuel*, **79**(11), 1371-1378.

Wang, B., Li, X., Xu, S., Paterson, N., Dugwell, D., Kandiyoti, R. 2005. Performance of Chinese coals under conditions simulating entrained-flow gasification. *Energy & Fuels*, **19**(5), 2006-2013.

Wang, G., Zhang, J., Shao, J., Liu, Z., Wang, H., Li, X., Zhang, P., Geng, W., Zhang, G. 2016. Experimental and modeling studies on CO 2 gasification of biomass chars. *Energy*, **114**, 143-154.

Wang, S., Wang, H., Yin, Q., Zhu, L., Yin, S. 2014. Methanation of bio-syngas over a biochar supported catalyst. *New Journal of Chemistry*, **38**(9), 4471-4477.

Wang, W., Padban, N., Ye, Z., Andersson, A., Bjerle, I. 1999. Kinetics of ammonia decomposition in hot gas cleaning. *Industrial & Engineering Chemistry Research*, **38**(11), 4175-4182.

Wang, Z., Mai, K., Kumar, N., Elder, T., Groom, L.H., Spivey, J.J. 2017. Effect of Steam During Fischer–Tropsch Synthesis Using Biomass-Derived Syngas. *Catalysis letters*, **147**(1), 62-70.

Wei, L., Kawamoto, K. 2013. Upgrading of simulated syngas by using a nanoporous silica membrane reactor. *Chemical Engineering & Technology*, **36**(4), 650-656.

Wei, L., Xu, S., Zhang, L., Zhang, H., Liu, C., Zhu, H., Liu, S. 2006. Characteristics of fast pyrolysis of biomass in a free fall reactor. *Fuel Processing Technology*, **87**(10), 863-871.

Werle, S. 2015a. Gasification of a dried sewage sludge in a laboratory scale fixed bed reactor. *Energies*, **8**(8), 8562-8572.

Werle, S. 2015b. Sewage sludge-to-energy management in eastern Europe: a Polish perspective. *Ecological Chemistry and Engineering S*, **22**(3), 459-469.

Wiedner, K., Rumpel, C., Steiner, C., Pozzi, A., Maas, R., Glaser, B. 2013. Chemical evaluation of chars produced by thermochemical conversion (gasification, pyrolysis and hydrothermal carbonization) of agro-industrial biomass on a commercial scale. *Biomass and Bioenergy*, **59**, 264-278.

Wolfesberger, U., Aigner, I., Hofbauer, H. 2009. Tar content and composition in producer gas of fluidized bed gasification of wood—Influence of temperature and pressure. *Environmental Progress & Sustainable Energy: An Official Publication of the American Institute of Chemical Engineers*, **28**(3), 372-379.

Xiong, X., Iris, K., Cao, L., Tsang, D.C., Zhang, S., Ok, Y.S. 2017. A review of biochar-based catalysts for chemical synthesis, biofuel production, and pollution control. *Bioresource Technology*.

Xiu, S., Shahbazi, A., Li, R. 2017. Characterization, Modification and Application of Biochar for Energy Storage and Catalysis: A Review. *Trends in Renewable Energy*, **3**(1), 86-101.

Xu, D., Lewis, R.S. 2012. Syngas fermentation to biofuels: Effects of ammonia impurity in raw syngas on hydrogenase activity. *Biomass and Bioenergy*, **45**, 303-310.

Xue, Y., Zhou, S., Brown, R.C., Kelkar, A., Bai, X. 2015. Fast pyrolysis of biomass and waste plastic in a fluidized bed reactor. *Fuel*, **156**, 40-46.

Yan, H.-m., Heidenreich, C., Zhang, D.-k. 1998. Mathematical modelling of a bubbling fluidised-bed coal gasifier and the significance of 'net flow'. *Fuel*, **77**(9-10), 1067-1079.

Yan, W.-C., Shen, Y., You, S., Sim, S.H., Luo, Z.-H., Tong, Y.W., Wang, C.-H. 2018. Model-based downdraft biomass gasifier operation and design for synthetic gas production. *Journal of Cleaner Production*, **178**, 476-493.

Yang, L., Ge, X. 2016a. Biogas and Syngas Upgrading. *Advances in Bioenergy*, **1**, 125-188.

Yang, L., Ge, X. 2016b. Chapter Three-Biogas and Syngas Upgrading. *Advances in Bioenergy*, **1**, 125-188.

Yao, D., Hu, Q., Wang, D., Yang, H., Wu, C., Wang, X., Chen, H. 2016. Hydrogen production from biomass gasification using biochar as a catalyst/support. *Bioresource Technology*, **216**, 159-164.

Yao, X., Yu, Q., Xie, H., Duan, W., Han, Z., Liu, S., Qin, Q. 2017. Syngas production through biomass/CO2 gasification using granulated blast furnace slag as heat carrier. *Journal of Renewable and Sustainable Energy*, **9**(5), 053101.

Yao, Z., You, S., Ge, T., Wang, C.-H. 2018. Biomass gasification for syngas and biochar co-production: Energy application and economic evaluation. *Applied Energy*, **209**, 43-55.

Yargicoglu, E.N., Sadasivam, B.Y., Reddy, K.R., Spokas, K. 2015. Physical and chemical characterization of waste wood derived biochars. *Waste Management*, **36**, 256-268.

Yazdanbakhsh, F., Alizadehgiashi, M., Bläsing, M., Müller, M., Sawada, J.A., Kuznicki, S.M. 2016. Cu-Cr-O functionalized ETS-2 nanoparticles for hot gas desulfurization. *Journal of Nanoscience and Nanotechnology*, **16**(1), 878-884.

Yazdanbakhsh, F., Bläsing, M., Sawada, J.A., Rezaei, S., Müller, M., Baumann, S., Kuznicki, S.M. 2014. Copper exchanged nanotitanate for high temperature H_2S adsorption. *Industrial & Engineering Chemistry Research*, **53**(29), 11734-11739.

You, F., Tao, L., Graziano, D.J., Snyder, S.W. 2012. Optimal design of sustainable cellulosic biofuel supply chains: multiobjective optimization coupled with life cycle assessment and input–output analysis. *AIChE Journal*, **58**(4), 1157-1180.

You, S., Ok, Y.S., Chen, S.S., Tsang, D.C., Kwon, E.E., Lee, J., Wang, C.-H. 2017a. A critical review on sustainable biochar system through gasification: Energy and environmental applications. *Bioresource Technology*.

You, S., Tong, H., Armin-Hoiland, J., Tong, Y.W., Wang, C.-H. 2017b. Techno-economic and greenhouse gas savings assessment of decentralized biomass gasification for electrifying the rural areas of Indonesia. *Applied Energy*, **208**, 495-510.

You, S., Wang, W., Dai, Y., Tong, Y.W., Wang, C.-H. 2016. Comparison of the co-gasification of sewage sludge and food wastes and cost-benefit analysis of gasification-and incineration-based waste treatment schemes. *Bioresource Technology*, **218**, 595-605.

Yuan, X., He, T., Cao, H., Yuan, Q. 2017a. Cattle manure pyrolysis process: Kinetic and thermodynamic analysis with isoconversional methods. *Renewable Energy*, **107**, 489-496.

Yuan, Y., Bolan, N., Prévoteau, A., Vithanage, M., Biswas, J.K., Ok, Y.S., Wang, H. 2017b. Applications of biochar in redox-mediated reactions. *Bioresource Technology*.

Zeng, X., Shao, R., Wang, F., Dong, P., Yu, J., Xu, G. 2016. Industrial demonstration plant for the gasification of herb residue by fluidized bed two-stage process. *Bioresource Technology*, **206**, 93-98.

Zhang, H., Zhang, Y., Zhu, Z., Lu, Q. 2016. Circulating fluidized bed gasification of low rank coal: Influence of O2/C molar ratio on gasification performance and sulphur transformation. *Journal of Thermal Science*, **25**(4), 363-371.

Zhang, L., Mi, M., Li, B., Dong, Y. 2013. Modification of activated carbon by means of microwave heating and its effects on the pore texture and surface chemistry. *Research Journal of Applied Sciences, Engineering and Technology*, **5**(5), 1836-1840.

Zhao, B., O'Connor, D., Zhang, J., Peng, T., Shen, Z., Tsang, D.C., Hou, D. 2018. Effect of pyrolysis temperature, heating rate, and residence time on rapeseed stem derived biochar. *Journal of Cleaner Production*, **174**, 977-987.

Zhao, L., Cao, X., Mašek, O., Zimmerman, A. 2013a. Heterogeneity of biochar properties as a function of feedstock sources and production temperatures. *Journal of Hazardous Materials*, **256**, 1-9.

Zhao, Y., Haddad, M., Cimpoia, R., Liu, Z., Guiot, S.R. 2013b. Performance of a Carboxydothermus hydrogenoformans-immobilizing membrane reactor for syngas upgrading into hydrogen. *International Journal of Hydrogen Energy*, **38**(5), 2167-2175.

Zhao, Y., Sun, S., Tian, H., Qian, J., Su, F., Ling, F. 2009. Characteristics of rice husk gasification in an entrained flow reactor. *Bioresource Technology*, **100**(23), 6040-6044.

Zwart, R.W., Boerrigter, H., van der Drift, A. 2006. The impact of biomass pretreatment on the feasibility of overseas biomass conversion to Fischer−Tropsch products. *Energy & Fuels*, **20**(5), 2192-2197.

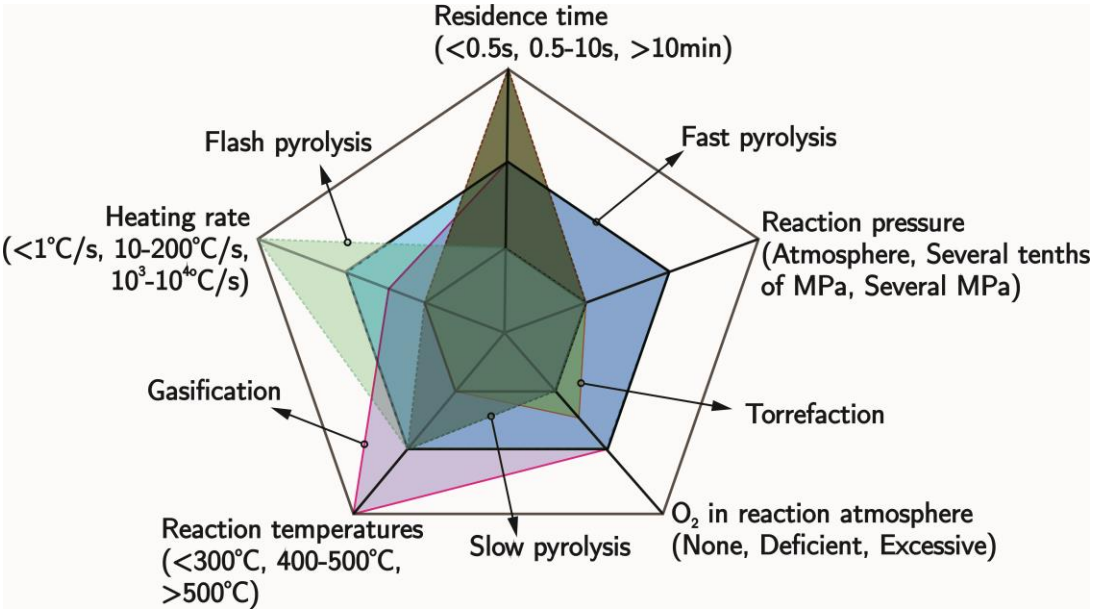

Figure 1. Differentiation of various thermochemical processes (slow pyrolysis, fast pyrolysis, flash pyrolysis, gasification, and torrefaction) in terms of reaction conditions (Asadullah et al., 2014; Brewer et al., 2011; Papari & Hawboldt, 2015; Patel et al., 2016; Sharma et al., 2015). Purple, grey, blue, light green, and dark green denotes gasification, slow pyrolysis, fast pyrolysis, flash pyrolysis, and torrefaction, respectively.

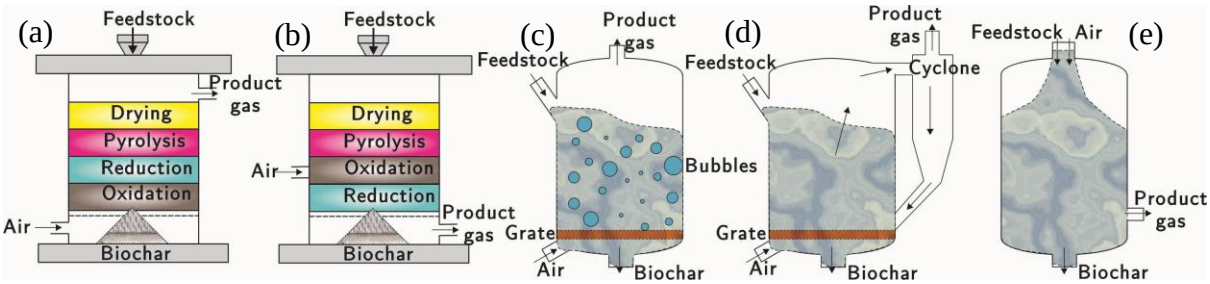

Figure 2. Five typical gasifier configurations: (a) updraft fixed bed, (b) downdraft fixed bed, (c) fluidized bed, (d) circulating fluidized bed, and (e) entrained flow.

Table 1. Feature comparison of different types of gasifiers

Type	Scale	Overall features	Sub-type	Specific features
Fixed bed	10 kW - 10 MW	• Poorer heat transfer and mixing • Problems such as slagging, bridging, and clinkering • Large feedstock particles and channeling effect • Non-uniform temperature distribution	Updraft	• Feedstock moisture content up to 50 wt.% • Unsuitable for feedstock with high volatile content • Feedstock ash content up to 15 wt.%
			Downdraft	• Low tar content in product gas (<1 g/m^3) • Feedstock moisture and ash contents smaller than 25 wt.% and 6 wt. %, respectively • Lower fixed carbon in biochar
Fluidized bed	5 - 100 MW	• Complete mixing and uniform temperature distribution • Wide range of applicable feedstock and particle size • Partial conversion of biochar • Post-stream separating biochar from bed particles	Bubbling bed	• Typical tar content less than 1 - 3 g/m^3 • Tar concentration decreased as temperature decreased and bed flow-rates decreases • Problems such as ash melting, sintering, and slagging by excessively high temperature • Defluidization by high alkali oxides content • High overall carbon conversion efficiency • Uniform quality biochar
			Circulating bed	• Long residence time • Bed material affecting biochar yield • Could be operated at low temperature (<750 °C) • Ash sintering issue mitigated
Entrained flow	>50 MW	• Short residence time (a few to tens of seconds) • High temperature (>1400 °C) and fine particle (<0.1 - 0.4 mm) • High carbon conversion (95 - 99%) and low biochar yield • Unsuitable for fibrous biomass • Feedstock particle mixed with water for facilitating feeding and H_2 production.		